BBA - Reviews on Cancer 1876 (2021) 188631

Contents lists available at ScienceDirect

BBA - Reviews on Cancer

journal homepage: www.elsevier.com/locate/bbacan

Review

A holistic view on c-Kit in cancer: Structure, signaling, pathophysiology and its inhibitors

Shelly Pathania [a], Olli T. Pentikäinen [b], Pankaj Kumar Singh [b,*]

[a] Department of Pharmaceutical Chemistry, ISF College of Pharmacy, Ghal Kalan, Ferozpur G.T. Road, Moga 142001, Punjab, India
[b] Integrative Physiology and Pharmacology, Institute of Biomedicine, Faculty of Medicine, University of Turku, FI-20520 Turku, Finland

ARTICLE INFO

Keywords:
c-Kit
Stem cell growth factor receptor
Melanoma
SCF
Kinases
Pathophysiology
c-Kit inhibitors

ABSTRACT

Receptor tyrosine kinases play an important role in many cellular processes, and their dysregulation leads to diseases, most importantly cancer. One such receptor tyrosine kinase is c-Kit, a type-III receptor tyrosine kinase, which is involved in various intracellular signaling pathways. The role of different mutant isoforms of c-Kit has been established in several types of cancers. Accordingly, promising c-Kit inhibition results have been reported for the treatment of different cancers (*e.g.*, gastrointestinal stromal tumors, melanoma, acute myeloid leukemia, and other tumors). Therefore, lots of effort has been put to target c-Kit for the treatment of cancer. Here, we provide a comprehensive compilation to provide an insight into c-Kit inhibitor discovery. This compilation provides key information regarding the structure, signaling pathways related to c-Kit, and, more importantly, pharmacophores, binding modes, and SAR analysis for almost all small-molecule heterocycles reported for their c-Kit inhibitory activity. This work could be used as a guide in understanding the basic requirements for targeting c-Kit, and how the selectivity and efficacy of the molecules have been achieved till today.

1. Introduction

The role of receptor tyrosine kinases in normal cellular function is essential, but also their dysfunction is known to play an essential role in cancer. Accordingly, much work has been conducted on these kinases. Optimistically, the efforts have resulted in several FDA-approved drugs against different members of this family [1–7]. Humans have 58 known receptor tyrosine kinases, categorized into 20 subfamilies. One of the prominent member of this family is c-Kit, also known as stem cell growth factor receptor [8]. It is one of the type III receptor tyrosine kinases and is known to play a critical role in the occurrence and proliferation of cancer [9]. It is a well-known cell surface receptor that binds to its physiological ligand, stem cell factor (SCF), also known as c-Kit ligand, leading to several physiological functions, such as homeostasis and melanogenesis [10]. Several studies have established that pigmentation disorders occur in the case of functional c-Kit aberration in both humans and mice. Additionally, inactivating heterozygous mutations in the Kit gene are attributed to piebaldism, a rare autosomal disorder characterized by congenital patchy depigmentation of the skin. Physiologically, the activation of c-Kit occurs *via* binding of SCF, leading to the homodimerization of the receptor, which results in a series of events involving transphosphorylation, auto-inhibitory interactions, and activation of multiple downstream effectors [11]. Although the overall outcome of c-Kit activation depends on the nature of the involved cell, several effector biomolecules have been reported to be activated, such as MAP kinases, Src family kinases, p85 subunit of PI3K, and phospholipase C-gamma [12].

Although c-Kit is a critical mitogen for melanocytes, in melanoma, it has been reported to be lost during disease progression [13,14]. Some other studies have also proposed insignificant levels of c-Kit in most melanoma cell lines. In contrast, *in-vitro* studies suggested that c-Kit may have a tumor-suppressing role, at least in melanoma [15]. Supporting this hypothesis, melanoma xenografts having lower levels of c-Kit expression have displayed higher metastatic potential, whereas abnormal levels of c-Kit expression in KIT-deficient lines were found to inhibit proliferation in these cells *in vivo* [16]. Conversely, dysregulation of c-Kit, including overexpression and gain of function mutations, have been reported in different types of cancer, such as gastrointestinal stromal tumors (GISTs; in 70–80% of the cases), small-cell lung carcinomas, and acute myeloid leukemia, exemplifying its clear oncogenic role [17,18]. Leukemia is one of the earliest cancers established to be correlated with c-Kit activating mutation [19,20]. In addition, c-Kit

* Corresponding author.
E-mail address: pankaj.singh@utu.fi (P.K. Singh).

https://doi.org/10.1016/j.bbcan.2021.188631
Received 30 July 2021; Received in revised form 8 September 2021; Accepted 28 September 2021
Available online 1 October 2021

mutations have been detected in unilateral ovarian dysgerminoma [21,22], melanoma [13,23], and others. Subsequent studies have disclosed that in a majority of the cases of systemic mastocytosis and other hematopoietic cancers, activating mutation in c-Kit is observed [24].

Expectedly the use of c-Kit inhibitors has provided novel insights for cancer treatment [25]. It has been reported that inhibiting c-Kit *via* kinase inhibitors, such as imatinib and related analogs, is a promising cancer-targeting approach [26]. However, several issues have also been identified concerning this strategy. First and foremost, imatinib resistance has been observed in many instances that treatment with imatinib results in c-Kit mutations leading to resistance [27]. Additionally, c-Kit is thoroughly expressed in normal tissues of the body, such as breast epithelial, vascular endothelial, sweat glands, and retinal astrocytes [28]; thus, every c-Kit mutation cannot be contemplated as a risk factor for the occurrence of cancer [29]. Therefore, targeting c-Kit, when it is the "driver" of the tumor, seems the best feasible option for cancer treatment. Lots of effort has been put into the development of targeted small molecule heterocycles against c-Kit, highlighting the need for a report on the work's current status in this direction. Appropriately, this work is a compilation of information about the structural attributes of this kinase target, its place in various signaling pathways, and various small molecule inhibitors developed to target c-Kit in cancer, which could be utilized to shape the directions of future research efforts.

2. Structure of c-Kit

The c-Kit receptor is encoded by a proto-oncogene present in the long-arm region of chromosome 4 (4q11–4q13) [30], spanning more than 34 kb of DNA. It maps to chromosome 12 in humans and chromosome 10 in the mouse and is encoded by nine exons in both humans and mice. The extracellular part of c-Kit is encoded by exons 2–9, while the transmembrane region is encoded by exon 10; the remaining exons encode the intracellular part of the receptor [11]. Similar to other members of class III of the RTK family, structurally, c-Kit consists of three domains: a hydrophobic transmembrane, an extracellular ligand-binding domain, and a cytoplasmic domain with tyrosine kinase activity [31]. c-Kit presents a canonical structure with two lobes and an active site in their interface [32]. It consists of 976 amino acids, having a core protein size of around 110 kDa. The extracellular domain contains 519 amino acid residues; the transmembrane domain consists of 23 amino acid residues; the intracellular 433 amino acid tail contains juxtamembrane and a tyrosine kinase domains connected by roughly 80 amino acid residues. Four c-Kit isoforms have been reported in humans; two isoforms have been reported in mice due to alternative mRNA splicing that encodes c-Kit. In both humans and mice, two of these isoforms differ from each other by the presence or absence of a tetrapeptide sequence (GNNK) in the extracellular juxtamembrane region of the encoded protein. An additional splice variant that differs by the presence or absence of a single serine residue in the kinase insert region of c-Kit also exists [11,33].

As the small molecule inhibitors are designed by focusing on the kinase domain, we will highlight its key structural attributes. The active site in c-Kit centers around the bound Mg^{2+} ion and ADP, which lies in the cleft between the N- and C-lobes. The bound conformation of ADP evidences that the adenine core resides in the hydrophobic pocket, forming H-bonds with Cys673 and Glu671 (Fig. 1). Additionally, the ribose sugar interacts with Asp677 and Arg796. Similar to the generally observed kinase fold, the kinase domain of c-Kit also folds with a COOH-terminal and NH_2-terminal lobe having the active site in the interface [34]. Further, a juxtamembrane domain is situated between COOH- and NH_2 -terminal lobes of the kinase domain. In the inactive state, the juxtamembrane region forms a hairpin loop that inserts into the active site and disrupts the regulatory process, suppressing its kinase activity and thereby acting as an autoinhibitory regulatory domain [35]. Moreover, in the inactive conformation, the Tyr823 present in the activation loop interacts with Asp792 in the active site, indicating a pseudo-substrate function. Upon binding of the physiological ligand (SCF), dimerization occurs, which leads to transphosphorylation. Tyr568 and Tyr570 of this juxtamembrane domain are phosphorylated, which in turn reorient the juxtamembrane domain, relieving it of its autoinhibitory conformation, which it acquires in an inactive state facilitating its catalytic function [36,37]. All these structural features establish the juxtamembrane domain as a critical regulatory feature. Another key observation is that in the active conformation of kinase structure, the Tyr823 of the activation loop is not phosphorylated, which agrees with another work disclosing that Y823F mutation does not impact kinase activity in c-Kit [38]. In the activation process of c-Kit, as studied by DiNitto et al., Tyr568 and Tyr570 in the juxtamembrane region are the first ones to be phosphorylated, followed by kinase insert; in contrast, the activation loop is phosphorylated near the end of the process [39]. Some of these phosphorylation sites in the juxtamembrane region of c-Kit, including Tyr547, Tyr553, Tyr568, Tyr570, Tyr703, Tyr721, Tyr730, Tyr823, Tyr900, and Tyr936, with SH2 (Src homology 2) domains, form docking sites for signaling molecules initiating signaling pathways. There are three distinct binding sites reported in binding pockets of c-Kit. There is one present in the first

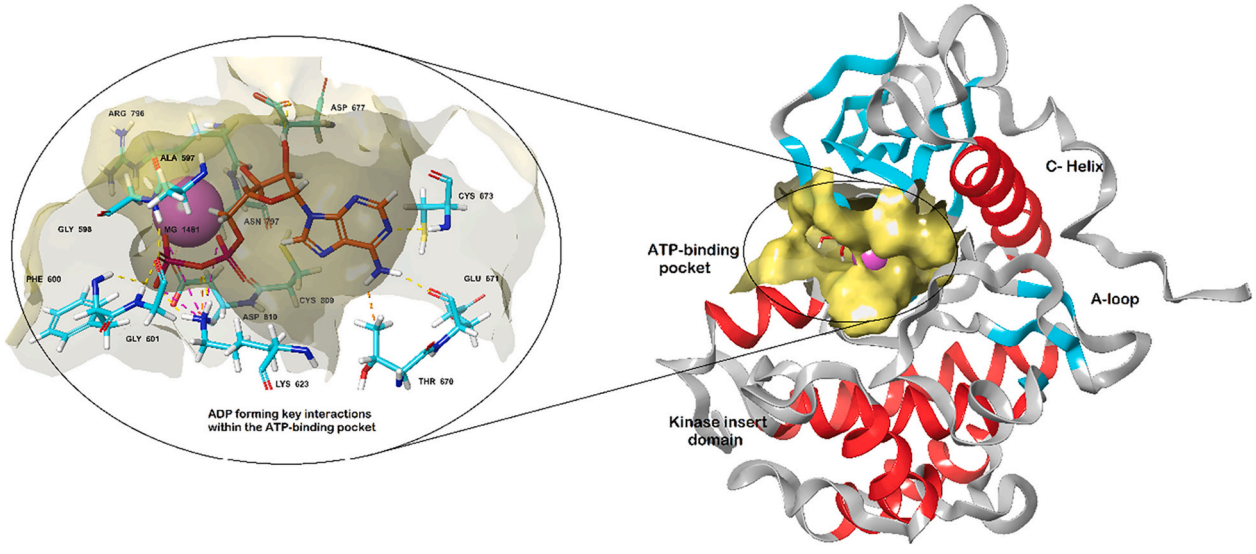

Fig. 1. 3-D structure of c-Kit along with the interaction diagram of ADP within the ATP-pocket.

immunoglobulin-like (Ig-like) domain, which consists of Asp72, Glu73, and Thr74, which interacts with the growth factor. Another is present in the second Ig-like domain that extends onto the linker region, which consists of Arg122, Ser123, Tyr125, Arg181, Ile201, Lys203, Arg205, and Glu198. The last is in the third Ig-like domain, consisting of Ser240, Ser241, Val242, Ser244, Tyr259, Asp260, Ser261, Trp262, His263, and Thr269 [40].

3. Physiological functions of c-Kit

c-Kit is a prominent component of cellular signaling in stem cells, where physiologically, it is involved in the crucial functions of cell maintenance and differentiation [41]. Prominent expression of c-Kit has been observed in stem cells, progenitor cells, and other cells with self-renewal potency [8]. It has been shown that c-Kit is present in hematopoietic cells, a stem cell type that divides asymmetrically and differentiates into various kinds of hematopoietic cell lineages (*e.g.*, macrophages, neutrophils, basophils, eosinophils, erythrocytes, T-cells, and B-cells) [42]. The levels of c-Kit expression are significant in the original hematopoietic cells; it diminishes after the differentiation step. Accordingly, although blood cells maintain proliferation upon differentiation, they lose the stemness and self-renewal ability [43]. Studies report that <1% of peripheral blood cells show expression of c-Kit, indicating its minimal role in differentiated blood cells. Another type of cell showing high expression of c-Kit includes mast cells. Upon complete differentiation, these cells rely on c-Kit-dependent signaling for survival, function, and growth [44]. Similarly, c-Kit is also involved in maintaining the immune system in adult animals. Germ cells, a type of progenitor cell, are also affected by c-Kit expression. Reports have disclosed the protective action of c-Kit mutations, *via* PI3K (phosphatidylinositide-3′-kinase)/AKT (Protein kinase B) pathway, on the germ cells towards apoptosis, followed by initiation of migration and proliferation [45]. Both over and underexpression of c-Kit have been reported problematic in mice, with overexpression leading to inactivation of PI3K, resulting in infertility [46] and underexpression leading to migration of melanocytes to the dermis causing pigmentation [47]. Furthermore, c-Kit is also involved in the normal functioning of cellular systems in the digestive and nervous systems. Studies have established the role of c-Kit in the development and function of interstitial cells of Cajal (ICC). With loss-of-function mutations in mice causing depletion of ICC, resulting in diseases such as slow transit constipation [48]. The expression of c-Kit in neuro-proliferative cells and its role in their development and function has also been reported. Especially in cases of injuries to the brain, c-Kit signaling plays a vital role in the migration of neural stem cells [49]. The role of c-Kit is also established in the functioning of cardiac stem cells (CSC). Several studies have reported that c-Kit$^+$ CSC cells, *bona fide* stem cells, improve the cardiac function and attenuate adverse left ventricular (LV) remodeling in both ischemic and non-ischemic cardiomyopathy [50]. c-Kit$^+$ CSC cells are also involved in several cardiovascular diseases, including acute myocardial infarction (AMI), ischemia/reperfusion (I/R) injury, chronic heart failure (CH), diabetic cardiomyopathy, aging myopathy, congenital heart disease (CHD), and anthracycline-induced cardiomyopathy [51,52]. Importantly, it has been suggested that imatinib, a well-known c-Kit inhibitor, is cardiotoxic and can lead to severe left ventricular dysfunction and heart failure, indicating cardiotoxicity risk with other c-Kit inhibitors as well [53]. Accordingly, a wide range of physiological functions dependent on the expression and proper functioning of c-Kit and loss of which can lead to several defects have been established [11].

4. c-Kit as a member of different signaling pathways

c-Kit participates in the signal transduction through different intracellular pathways (Table 1):

Table 1
List of details regarding c-Kit downstream signaling pathways.

S. No.	Signaling pathway	Location	Functional outcome
1.	PI3K pathway	Fibroblast cells and hematopoietic cells	Cellular survival and proliferation
2.	JAK/STAT pathway	Hematopoietic cells	Activate transcription of a variety of genes
3.	Src family kinase pathway	Hematopoietic progenitor cells	Chemotaxis and proliferation
4.	MAPK pathway	Hematopoietic cells	Gene transcription, cell differentiation

4.1. PI3K pathway

c-Kit, upon binding of SCF, is involved in the activation of the PI3K pathway, which involves phosphorylation of inositol core of the lipids in the cell membrane *via* PI3K [54]. PI3K activation occurs directly by binding to Tyr721 in c-Kit and indirectly by binding to GAB2, a tyrosine-phosphorylated adaptor protein phosphorylated through Grb2-dependent recruitment to the receptor followed by Src-mediated phosphorylation. As GAB2 expression differs between cell types, and it interacts differently with different isoforms of c-Kit, indirect activation allows for increased complexity. This phosphorylation leads to an increase in negative electric potential across the lipid, resulting in an interaction between PIP3 and pleckstrin homology (PH) domain-containing proteins. Consequently, the PH domain protein activates AKT, which is crucial for the apoptosis ability of SCF [55]. Activated Akt promotes cell survival in different ways, including phosphorylation of Bad and Foxo and the activation of nuclear factor kappa-light-chain-enhancer of activated B cells (NF-κB). Bad, a protein involved in the control of cytochrome *c* release from the mitochondria, heterodimerizes, thereby neutralizing the anti-apoptotic proteins Bcl-X_L or Bcl-2 in the absence of survival signals. Bcl-X_L antagonizes the pro-apoptotic Bax protein-blocking cytochrome *c* release and consequently apoptosis. In addition, PI3K also plays an essential function in SCF-induced proliferation, regulation of the actin cytoskeleton, cell growth, and tumorigenicity (Fig. 2) [56].

4.2. MAPK pathway

The other signaling pathway stimulated by c-Kit is the mitogen-activated protein kinase (MAPK) pathway [57]. c-Kit in this signaling pathway recruits Sos (guanine exchange factor) to the small Ras GTPase (a GTP to GDP converter), which binds to Ras, the first member of the MAPK signaling pathway, resulting in a conformational change in RAS that allows it to interact with its downstream effectors [58]. Interestingly in c-Kit, Tyr703 and Tyr936 are primarily responsible for the direct interaction with the stable complex of Sos [59]. Sos exists in a complex with Grb2, which, in turn, associates *via* its SH2 domain with protein tyrosine phosphatase SHP-2, a downstream signal transduction molecule. Upon activation of Ras, the downstream effector Raf, a serine/threonine kinase, is translocated to the plasma membrane, where it activates *via* phosphorylation and de-phosphorylation. The next member of the pathway, MEK, is phosphorylated and activated *via* Raf, followed by activation of ERK, resulting in altered gene expression and protein activity (Fig. 2) [60,61]. Activated ERKs dimerize and translocate to the nucleus; downstream ERK1/2 proteins include transcription factors, such as c-Fos and Elk-1, while cytoplasmic substrates include Rsk. Interestingly some studies have disclosed a critical role of SFKs in ERK1/2 activation, revealing a cross-talk mechanism between the different downstream signaling pathways of c-Kit.

4.3. Src family kinase

Another signaling pathway that c-Kit executes its physiological

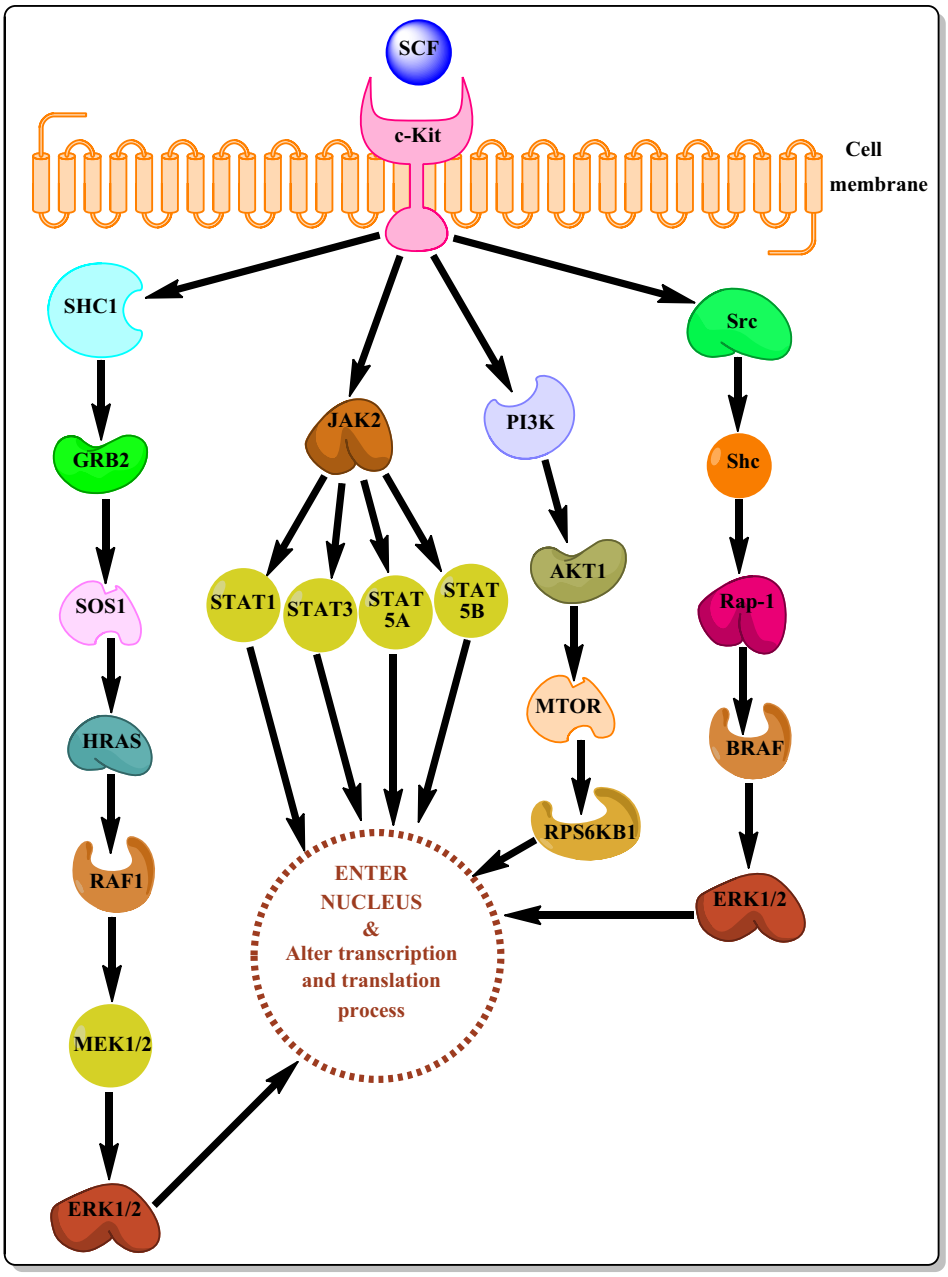

Fig. 2. The layout of different signaling pathways involving c-Kit (MAPK, JAK/STAT, PI3K, and Src kinase pathways).

action is the Src family kinases (SFKs) [58]. These are cytoplasmic tyrosine kinases and are involved in various vital cellular functions. One study involving phenotypic analysis on mutant c-Kit mice revealed that SFKs are prominently involved in c-Kit signaling in the lymphocytes [62]. Upon phosphorylation, Tyr568 and Tyr-570 of c-Kit interact with the SH2 domain in SFK, resulting in the opening of the structure and increased catalytic activity. It is considered that phosphatase SHP2 also plays an important role in this pathway by de-phosphorylating PAG (a transmembrane protein) and blocking Csk (a negative SFK regulator) recruitment. Upon activation, SFK has been reported to be involved in several signaling pathways. SFK signaling has been implicated in promoting cell migration *via* phosphorylation of FAK, which regulates focal adhesions. It has also been suggested that activation of SFK is involved in p38 MAPK activation and Ca^{2+} influx, which promote ERK1/2 activation and cell migration. Although the role of SFKs in c-Kit internalization and their activation *via* c-Kit has been established, the exact function of this activation in the pathway is not known [63]. SFKs play a vital role in SCF-induced chemotaxis and proliferation in primary hematopoietic progenitor cells. Furthermore, it has been demonstrated that SFKs affect the downstream pathways of c-Kit; any failure in the SFK signaling pathway results in severe complications, such as pigmentation, splenomegaly, and improper mast cell development (Fig. 2) [64].

4.4. JAK/STAT pathway

Another signaling pathway involving activation *via* c-Kit is the JAK/STAT pathway. Downstream of JAKs are the signal transducers and activators of transcription (STATs). c-Kit results in the permanent phosphorylation of all three, STAT1, STAT3, and STAT5, proteins with transcriptional activity [65]. The phosphorylation could be either intrinsic or by the receptor-associated JAK tyrosine kinase. STATs, a class of transcription factors, possess DNA-binding domains, an SH2 domain, and a trans-activating domain. Upon phosphorylation, STATs dimerize through phospho-tyrosine interaction within their SH2

domains and then translocate to the nucleus, where they regulate gene expression. It has been suggested that JAK2 is activated downstream of c-Kit and not JAK3. It has also been reported that JAK2 is also required to differentiate c-Kit^{+} progenitor cells into mast cells. Overall, the influence of c-Kit on the activation and molecular functions of the above-mentioned signaling pathways and cellular proteins varies considerably depending on the nature of the involved cells. More often than not, c-Kit functions in close coordination with other growth factors and cytokines (Fig. 2) [66].

5. Pathophysiological role: c-Kit and cancers

As discussed above, c-Kit is involved in several cellular functions, such as proliferation; expectedly, several studies have correlated dysregulation in c-Kit functions with different types of cancer [67]. Such dysregulations may occur for multiple reasons, including gain-of-function or loss-of-function mutations, other point mutations, *etc.* One of the initial studies disclosing the role of c-Kit in cancer identified it as a retroviral oncogene. To date, the role of c-Kit based on overexpression or mutations has been established in several cancers, including melanoma, thyroid carcinoma, and breast cancer [68,69]. More specifically, an activating mutation L576P in c-Kit is reported to be responsible for a small subset of metastatic melanoma cases [70]. In some GIST cases, other activating mutations such as D816V and V560G are considered the cause of tumorigenesis, and expectedly c-Kit inhibition by imatinib has been found to increase patient survival by 70%–80% after two years [71]. As in GIST, similar activating mutations, including V560G in the juxtamembrane region and D816V in the tyrosine kinase domain, are also detected and held responsible in mast cell leukemia (Table 2) [72,73].

Furthermore, mutations in c-Kit are also observed in the proliferating cases of systemic mastocytosis. Essentially, such mutations lead to induced c-Kit dimerization and eventually result in the activation of kinase domains. While the mutations on the kinase domain include the replacement of aspartic acid residues with asparagine, tyrosine, or histidine residues, resulting in ligand-independent activation [74]. The outcome of these mutations depends on the signaling pathway activated by the c-Kit—however, other types of cancer are caused by overexpression of c-Kit and its physiological ligand [11]. The most common ones involving overexpression of c-Kit include colorectal carcinoma, small-cell lung carcinoma, neuroblastoma, and malignant mesothelioma [74]. Expectedly several molecules have been designed to target c-Kit, but most of them are multi-targeting inhibitors. Almost all the FDA-approved drugs targeting c-Kit are also multi-targeting kinase inhibitors. Although selective inhibition of c-Kit is extremely challenging, it offers improved efficacy in the cancer cases with c-Kit mutations as the "driver" (*e.g.*, GISTs). Alternatively, multi-target c-Kit inhibitors are helpful in cases of uncontrolled proliferation, having other kinases, such as AML, at play [75]. Therefore, the impact of selective inhibition of c-Kit greatly depends on the complex pathophysiology and nature of the tumors.

Table 2
List of c-Kit mutations reported for their role in different types of cancer.

S. No.	c-Kit mutation	Impact	Protein effect	Related cancer
1.	E490K	Missense	Unknown	Thymic Carcinoma
2.	W557R	Missense	Unknown	Thymic Carcinoma, Melanoma
3.	V559A	Missense	Gain of function	Thymic Carcinoma, Gastrointestinal stromal tumor, Melanoma
4.	V560del	Deletion	Gain of function	Thymic Carcinoma, Melanoma, Gastrointestinal stromal tumor
5.	V560G	Missense	Gain of function	Gastrointestinal stromal tumor, Mastocytosis
6.	L576P	Missense	Gain of function	Thymic Carcinoma, Melanoma
7.	K642E	Missense	Gain of function	Melanoma, Gastrointestinal stromal tumor, acute lymphoblastic leukemia
8.	V654A	Missense	Unknown	Melanoma
9.	D816H	Missense	Gain of function	Melanoma, Acute Myelogenous Leukemia
10	D816V	Missense	Gain of function	Melanoma, Gastrointestinal stromal tumor, Mastocytosis, Acute Myelogenous Leukemia
11.	D820E	Missense	Unknown	Thymic Carcinoma,
12.	A829P	Missense	Gain of function	Melanoma, Gastrointestinal stromal tumor

6. Inhibitors of c-Kit as anti-cancer agents (Table 3)

In 2011, Patel et al. reported design, synthesis, and evaluation of pyridyl and phenyl analogs of OSI-930, a reported dual inhibitor of c-Kit and KDR (kinase insert domain receptor) [76], to better understand the binding site characteristics. The study revealed that compound **1**, an aminopyridyl derivative, showed 91% inhibition of c-Kit at 10 μM with weak inhibition of other kinases (Fig. 3). The inhibitory data of the compounds highlighted the importance of the H-bond acceptor in the core of OSI-930 [76]. Compounds with similar structural features as OSI-930, except for the pyridyl nitrogen atom, showed weaker inhibition of c-Kit. While *p*-hydroxy derivative, which could mimic the H-bond acceptor of OSI-930, showed improved activity compared to derivatives without the H-bond acceptor feature, it is still a weaker inhibitor than OSI-930 [77].

In 2011, Davies et al. explored the diaminotriazole scaffold for the development of potent and selective dual inhibitors of FLT3/c-Kit for the management of AML (Acute Myeloid Leukemia). Out of all, compound **2** showed potent and selective enzymatic and cell-based inhibitory potential against both c-Kit and FLT3. The design of these compounds was based on mimicking the flat, hydrophobic nature of the adenine pocket (Fig. 4). The selectivity of designed compounds was attributed to their steric interaction with Cys695, which is present in both FLT3 and c-Kit, while other kinases have proline in the structurally equivalent position. Compound **2** was also found to be cytotoxic against cancer cell lines such as MV-411, having the expression of c-Kit and FLT3, with IC_{50} between 1 and 5 nM. The most potent compound also showed strong efficacy against the Ba/F3-FLT3-ITD leukemia mouse model with a good pharmacokinetic profile [78]. In the same year, Heidary et al. reported the >100-fold selectivity of **2** (VX-322), a low nanomolar inhibitor of FLT3 and c-Kit, against the other kinases such as PDGFR-β and FMS. More importantly, **2** also showed an improved pharmacokinetic profile over other compounds of the pool with only a 5-fold shift in potency in the presence of 20% human serum. The study also indicated that compounds with dual inhibitory potency fared better against primary AML patient blast cells than single kinase inhibitors. Overall, **2** provided an improved pharmacological and selectivity profile for the treatment of AML [79].

In 2012, Almerico et al. attempted to establish the correlation between structural features and inhibitory activity for c-kit inhibitors employing 3D-QSAR pharmacophore modeling. In the study, a pharmacophore model containing one H-bond donor feature with four aromatic features was generated and validated. The volume occlusion maps indicated that inhibitory potential is correlated with the donor atoms in the aromatic rings of the core, which form the H-bond interaction within the catalytic domain. Test set prediction and the screening of active inhibitors from a known database were performed to validate the obtained model. Overall, the generated model might be utilized to screen more potent c-Kit inhibitors from query databases [80].

In 2013, Duveau et al. synthesized analogs of nilotinib to investigate the effects of trifluoromethyl substituent on its pharmacological profile. They substituted trifluoromethyl position with fluorine substituent, methyl substituent, and kept unsubstituted. Binding pocket analysis disclosed that in the case of trifluoromethyl (nilotinib) and methyl (**3**), the compounds fit tightly in the pocket of Abl. While in the case of c-Kit, due to the presence of a larger hydrophobic pocket, all mentioned

Table 3
List of c-Kit inhibitors currently developed along with the type of cancer cell line or animal models of cancer employed.

S. No.	Compound ID[a]	2D structure	Cell line/animal model used	IC_{50} against c-Kit
1.	1	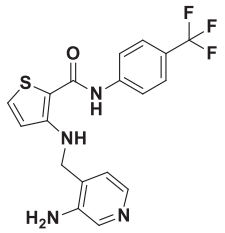	[b]	91% inhibition at 10 μM
2.	2	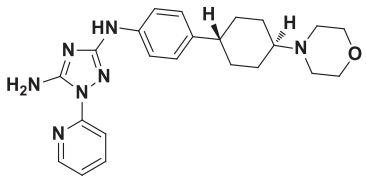	MV-411 cell line, Ba/F3-FLT3-ITD leukemia mouse model	1 nM
3.	3	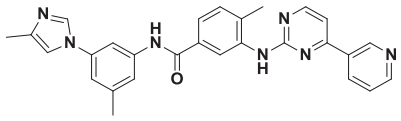	[b]	54.94 nM
4.	4	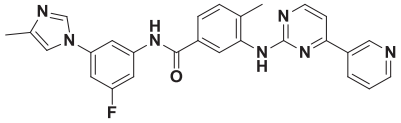	[b]	9.96 nM
5.	5	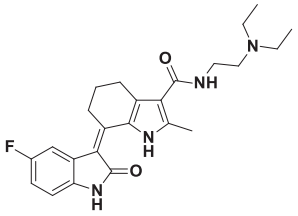	BXPC-3, T24, BGC, HEPG2, and HT29 cell lines	2.4 nM
6.	6	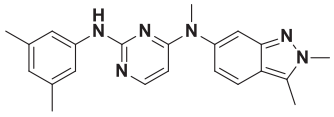	[b]	40 nM
7.	7	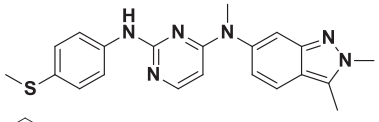	[b]	71 nM
8.	8	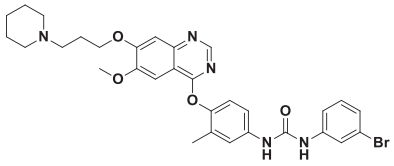	PC3, HT29, and MCF7 cell lines	9 nM
9.	9	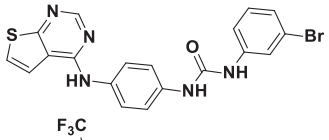	[b]	1 nM
10.	10	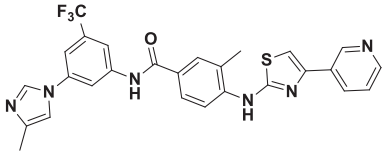	MCL cell line	138 nM

(*continued on next page*)

Table 3 (*continued*)

S. No.	Compound ID[a]	2D structure	Cell line/animal model used	IC_{50} against c-Kit
11.	11	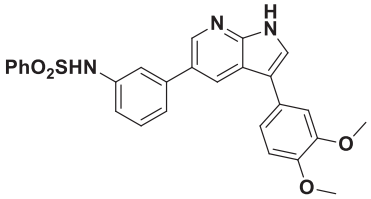	HMC-1.2 cell lines (V560G, D816V),	346 nM
12.	12	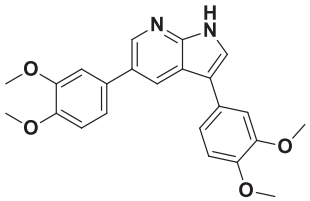	HMC-1.2 cell lines (V560G, D816V),	2.1 nM
13.	13	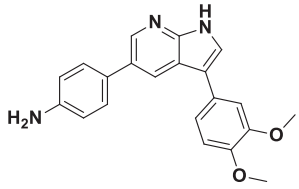	[b]	1.6 nM
14.	14	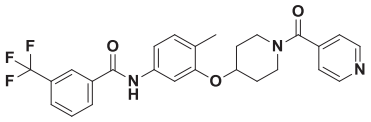	GIST-882, GIST-48B, K562, KU812, MEG-01, MV4-11 and HL-60 cell lines	99 nM
15.	15	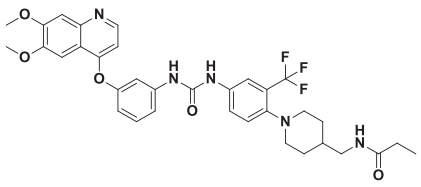	GIST-882, GIST-48B, K562, KU812, MEG-01, MV4-11 and HL-60 cell lines	33 nM
16.	16	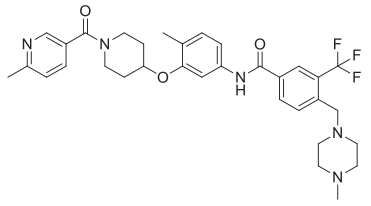	K562 and GIST-T1 cell lines	75 nM
17.	17	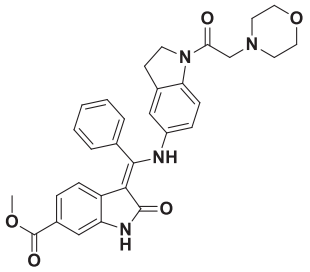	Bleomycin (BLM)-induced mouse pulmonary fibrosis model	10 nM
18.	18	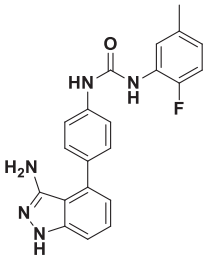	GIST-T1, GIST-882 cell lines and BaF3-TEL-cKIT-T670I isogenic cell inoculated xenograft mouse model	35 nM

(*continued on next page*)

Table 3 (*continued*)

S. No.	Compound ID[a]	2D structure	Cell line/animal model used	IC_{50} against c-Kit
19.	19	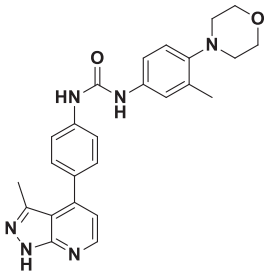	GIST-T1, GIST-882 cell lines and BaF3-TEL-cKIT-T670I isogenic cell inoculated xenograft mouse model	2.4 nM
20.	21	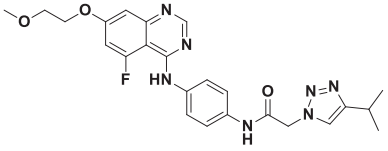	A panel of Ba/F3 cell lines and mouse allograft tumor models using Ba/F3 lines	16 nM
21.	22	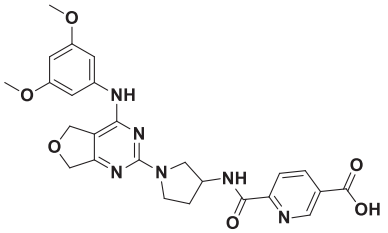	fibroblast-like synoviocytes and mouse bone marrow-derived mast cells	18.6 μM
22.	23	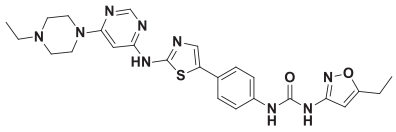	GIST882, GIST430, GIST48 cell lines and GIST430 xenograft mouse models	82 nM
23.	26	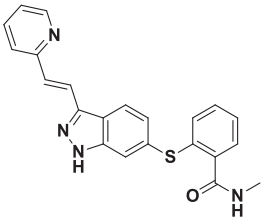	GIST-T1, GIST-882 and GIST-T1-T670I cell lines	108 nM
24.	27	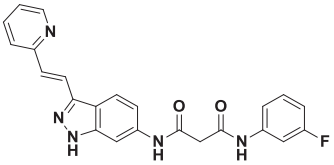	GIST-T1, GIST-882 and GIST-T1-T670I cell lines	44 nM
25.	28	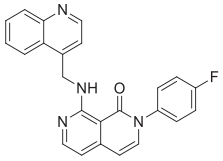	[b]	8.5 nM
26.	29	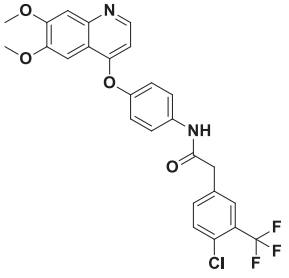	BaF3- tel-c-Kit, BaF3-tel-c-Kit-T670I, GIST-T1, GIST-882, GIST-T1-T670I, GIST-5R and GIST-48B cell lines	4 nM

(*continued on next page*)

Table 3 (*continued*)

S. No.	Compound ID[a]	2D structure	Cell line/animal model used	IC_{50} against c-Kit
27.	30	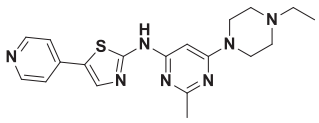	GIST-T1, MOLM-13, GIST882, GIST48, GIST430 cell lines and GIST430 xenograft mice models	56 nM
28.	37	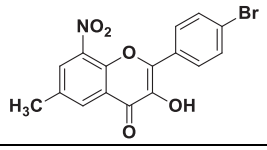	A375, SK-Mel-28, A431 and UWBCC1 cell lines	90 nM

[a] Compound ID as per discussion in this paper.
[b] Only *in-vitro* enzymatic data against c-Kit was available for these molecules.

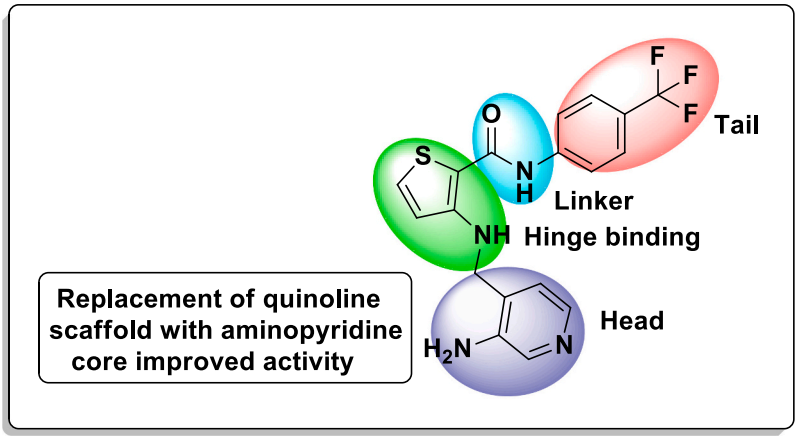

Fig. 3. The pharmacophoric description along with SAR analysis of compound **1** for c-Kit inhibitory activity.

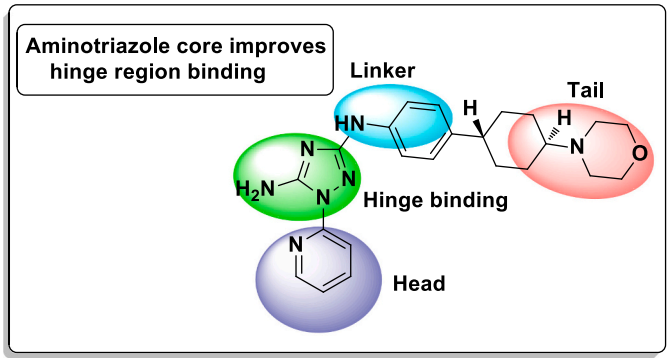

Fig. 4. The pharmacophoric description along with SAR analysis of compound **2** for c-Kit inhibitory activity.

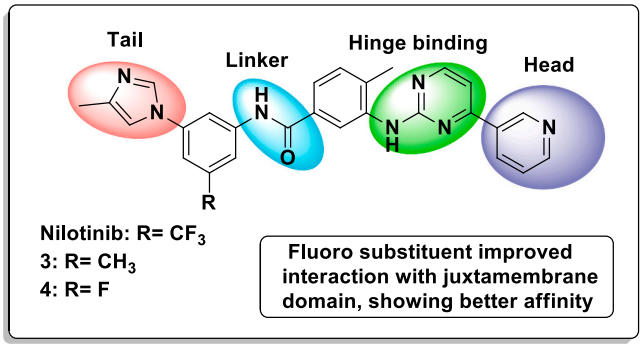

Fig. 5. The pharmacophoric description along with SAR analysis of compounds **3** and **4** for c-Kit inhibitory activity.

derivatives fit well in the catalytic domain. However, due to the interactions with the juxtamembrane domain, compound **4** with fluorine showed a high binding affinity towards c-Kit (Fig. 5). This particular observation highlighted the possibility of optimizing the selectivity of the compounds towards specific members of a highly related class of kinases. In this case, a small substitution from methyl to fluorine increases affinity for the compound towards c-Kit allowed fine-tuning of the activity profile of the kinase inhibitors [81].

In 2013, Ding et al. designed and synthesized 3-pyrrolo[*b*]cyclohexylene-2-dihydroindolinone derivatives. Expectedly, the compounds were found to possess significant inhibitory activity against multiple kinases, including VEGFR-2, PDGFR-ß, and c-Kit. The SAR analysis highlighted that the structural modifications on the phenyl ring of indolin-2-ones altered the potency of the compounds significantly (Fig. 6). Out of all, compound **5** exhibited significant inhibitory potential against all target kinases. Molecular modeling analysis of the most potent compound revealed the significance of indolin-2-one core in maintaining H-bonds interactions in the ATP binding site. The designed compounds also possessed good anti-proliferative potential against several cancer cell lines such as BGC, HEPG2, and HT29 [82].

In 2014, Qi et al. designed and synthesized analogs of pazopanib by substituting terminal benzene and indazole rings of pazopanib as multi-targeting kinase (VEGFR-2, PDGFR-α and c-Kit) inhibitors. SAR analysis indicated a correlation between the kinase inhibitory potential of the compounds and electronic and steric effects of the substituents in the analogs. Out of all, in comparison to pazopanib, compound **6** exhibited

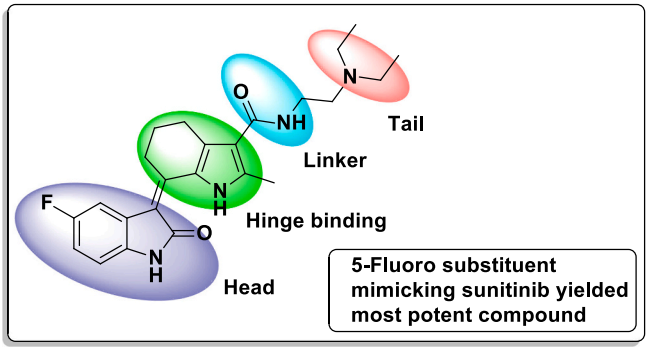

Fig. 6. The pharmacophoric description along with SAR analysis of compound **5** for c-Kit inhibitory activity.

superior inhibitory potential against all target kinases (Fig. 7). Additionally, compound **7** also showed sub-nanomolar range inhibitory potential against c-kit kinase, highlighting that the core of pazopanib with substituents of altered electronic potential impacts their binding affinity for c-Kit [83].

In 2014, Ravez et al. evaluated the multi-kinase inhibitory potential of 7-aminoalkoxy-4-aryloxy-quinazoline urea derivatives against VEGFR, PDGFR-β, and c-Kit. SAR analysis indicated that inserting a basic side chain in the methoxy group (diethylaminoalkoxy, piperidinoalkoxy, or pyrrolidinoalkoxy) at the 7th position of the quinazoline nucleus improves the kinase inhibitory potential of the synthesized compounds (Fig. 8). A significant improvement in the anti-proliferative potential was observed with selectivity towards cancer cell lines (PC3, HT29, and MCF7) over normal cells. Out of all, compound **8** showed potent anti-proliferative potential and better inhibition of endothelial cell invasion in comparison to the reference [84]. Next year, in 2015, the same group reported the discovery of selective and potent c-Kit inhibitors with preliminary biological evaluation. They developed a library of thieno and tetrahydrobenzothieno-pyrimidines and evaluated their multi-kinase inhibitory potential. Interestingly, it was observed that the 4-aryloxy derivatives have multi-kinase (VEGFR, PDGFR-β, and c-Kit) inhibitory potential while aniline analogs were found to be highly selective and potent inhibitors of c-Kit with nanomolar range IC_{50} values (Fig. 8). Out of all, the most potent compound, **9**, was found to possess selective c-Kit inhibitory potential with c-Kit IC_{50} = 1 nM. This lead molecule provided a novel architecture for the development of c-Kit inhibitors; however, initial results on cancer cell lines showed low inhibitions, highlighting the need to optimize the pharmacokinetic profile of the lead molecule [85].

In 2014, Jin et al. disclosed the identification of a kinase inhibitor, 126,332 (**10**), with the potential to inhibit cell proliferation in cells with imatinib-resistant KIT mutation (Fig. 9). It is claimed to act *via* blockade of KIT phosphorylation and its downstream signaling. 126,332 was also found to inhibit proliferation in cells with c-Kit having D816V mutation.

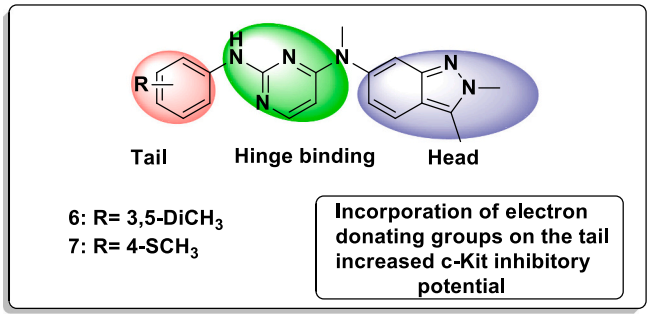

Fig. 7. The pharmacophoric description along with SAR analysis of compounds **6** and **7** for c-Kit inhibitory activity.

Interestingly, 126,332 showed equal levels of apoptosis in both imatinib-resistant and -sensitive cells. It also induced apoptosis in MCL cells, whereby decreased levels of apoptosis-related proteins regulated by transcriptional factor Stat3 and Stat5, were observed [29]. Along with inhibition of c-Kit activity, they also reported decreased levels of both nuclear and cytosolic β-catenin, which are known to be down-regulated upon silencing KIT [86].

In the same year, Lee et al. worked on tailoring a 7-azaindole-based hit (**11**) by following a structure-based *de novo* designing approach to target D816V mutant c-Kit. SAR analysis of the tailored compounds revealed that 7-azaindole derivatives having a 3,4-dimethoxybenzene ring at 3rd position with a polar aromatic ring at 5th position results in potent and selective c-Kit inhibitors with D816V mutation, with some even being in the nanomolar range (Fig. 10). The compounds were also found to possess 100-fold higher potency against mutant in comparison to wild-type c-Kit. Further, *in-silico*-assisted decomposition analysis revealed that decreasing the desolvation cost involved in the complexation of these molecules within the catalytic domain of c-Kit may improve their binding affinity and, in turn, improve their potency. Upon further experimental validation, out of all, four compounds were found to inhibit cell proliferation in imatinib-resistant cells in sub-micromolar concentrations. Out of all, compound **12** was also found to possess the most potent anti-cancer activity in imatinib-resistant cells [87]. Continuing their work, the same group in the same year studied the inhibitory activity and high selectivity of 7-azaindole-based molecules against D816V mutant c-Kit. Building on the previous work, they modified the scoring function taking into account the effects of ligand solvation on protein-ligand association and selected the hits with good binding affinity scores. The designed 7-azaindoles were synthesized and subjected to biological evaluation, which other than reiterating the previously known fact that 7-azaindole derivatives with a 3,4-dimethoxybenzene ring at 3rd position and a polar aromatic ring at 5th position are potent D816V mutant c-Kit inhibitors, also disclosed the critical role of the bidentate H-bond between the 7-azaindole moiety and Cys673 of the catalytic domain of c-Kit. Dynamic stability of this interaction was found to be directly correlated with the binding affinity of the designed molecules (Fig. 10). Out of all, compound **13** was most potent and can be considered a lead structure, specifically to inhibit the D816V mutant c-Kit [88].

In 2015, Chaudhari and Bari developed a pharmacophore and 3D QSAR model for c-Kit inhibitory activity *via* a series of indolin-2-one derivatives with well-defined c-Kit inhibitory activity. The generated pharmacophore model consisted of five features, including two aromatic ring features, one hydrophobic feature, one H-bond acceptor feature, and one H-bond donor feature. The statistical validation of the model indicated it to be robust and significant with R^2 = 0.9378 and Q^2 = 0.7832. External validation (Y-randomization and 'goodness-of-hits' approach) further improved the confidence in the predictive power of the model. Pharmacophore model validation was followed by molecular docking experiments, which indicated a significant correlation between the results of molecular docking and the developed model. It also highlighted the significance of H-bond interactions with Cys673 and Glu671 for the binding affinity in the catalytic domain of c-Kit. Finally, virtual screening of the ZINC database was performed utilizing the generated pharmacophore model and molecular docking experiments, which led to the selection of five hits with putative c-Kit inhibitory activity. The predicted ADME profile of the hits was also in the acceptable range [89].

In 2016, Wang et al. explored imatinib's core to design hybrid type II inhibitors, consequently leading to the discovery of selective c-Kit inhibitor, **14**. Imatinib is known to have activity against ABL kinase; however, **14** did not show any ABL kinase inhibitory activity. SAR analysis indicated that terminal pyridine was responsible for selectively retaining c-Kit activity over ABL. Also, incorporation of methyl substituent at the 4th position of the benzene enhanced 6-fold c-Kit activity (Fig. 11). Additionally, **14** was devoid of any FLT3 kinase inhibitory

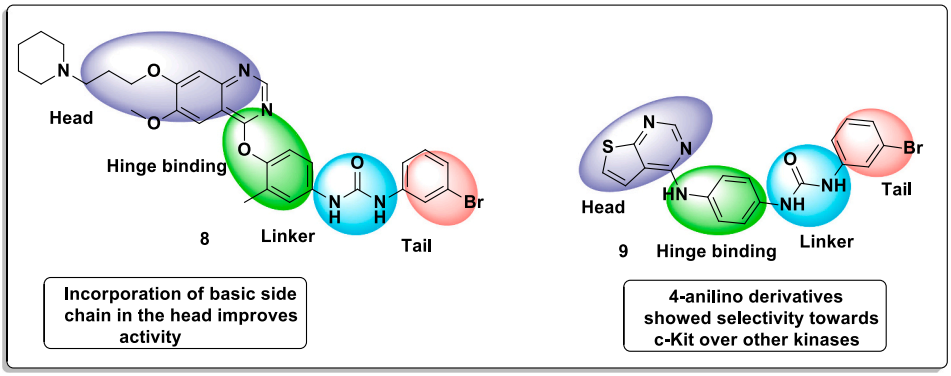

Fig. 8. The pharmacophoric description along with SAR analysis of compounds **8** and **9** for c-Kit inhibitory activity.

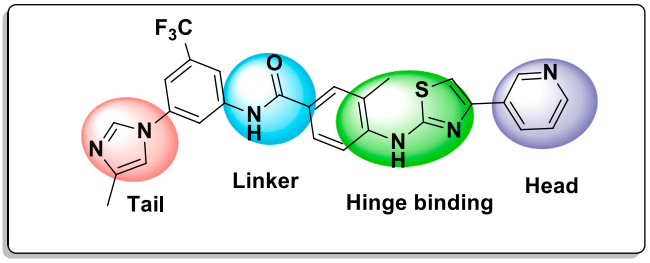

Fig. 9. Pharmacophoric description of compound **10** for c-Kit inhibitory activity.

activity; however, detailed screening showed its inhibitory potential against DDR1, PDGFRβ, and CSF1-R kinase. Molecular docking analysis of **14** in the catalytic domain of c-Kit showed a typical type II binding mode (DFG motif out). Differently from imatinib, **14** showed H-bond between terminal pyridine and piperidine with Cys673 in the hinge binding area. Further, the cell proliferation assays indicated that **14** showed potent inhibition of cell proliferation in c-Kit-dependent GISTs cancer cells. It is also worth mentioning that in the rat models, **14** showed an acceptable pharmacokinetic profile [90].

Similarly, in 2016, Li et al. attempted to discover quinoline-based type II inhibitors of c-Kit to manage c-Kit-expressed GIST. The study identified compound **15,** which showed potent inhibitory potential in both wild-type c-Kit and T670I-mutant c-Kit expressing GIST cancer cells. SAR analysis disclosed that increasing the substituent size coupled to urea moiety by using *N*-(piperidin-4-ylmethyl)propionamide leads to improved activity against wild type c-Kit while retaining activity against T670I mutant c-Kit (Fig. 12). Further, molecular modeling analysis revealed that **15** formed required interactions in the catalytic domain of c-Kit, including H-bond with Cys673, Glu640, and Asp810. More importantly, in the case of T670I mutant c-Kit, the O-bridged phenyl ring of **15** orients in such a manner that it provides enough room for the bulky isoleucine, expectedly resulting in its potency against T670I mutant [91,92].

In 2016, Wang et al. attempted to design type II c-Kit inhibitors *via* a hybrid structure-based drug design approach. The study led to the identification of compound **16** having credible potency against BCR-ABL and c-Kit. SAR analysis revealed that the 4-methylnicotinoyl group imparts both selectivity window and improved potency to **16** (Fig. 13). Molecular modeling analysis revealed that **16** orients distinctly in the hinge region with amide oxygen serving as the H-bond donor. Detailed biological experiments suggested that **16** also inhibits other kinases in the pool, including VEGFR, PDGFRα/β, and CSF1-R kinases. More

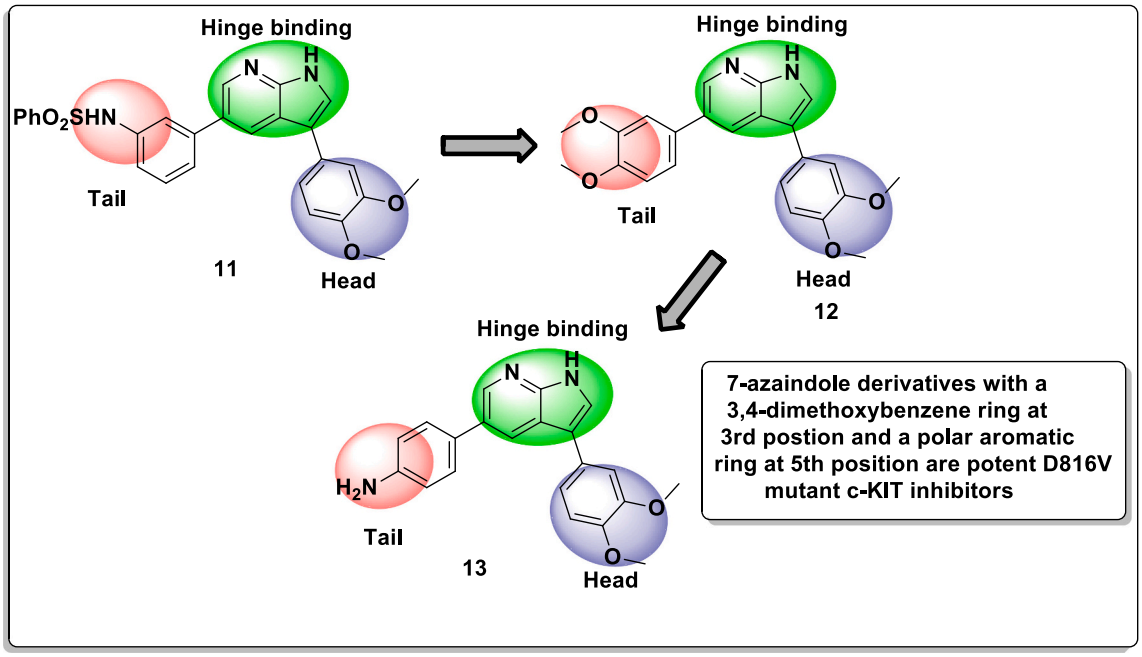

Fig. 10. The pharmacophoric description along with SAR analysis of compounds **11, 12,** and **13** for c-Kit inhibitory activity.

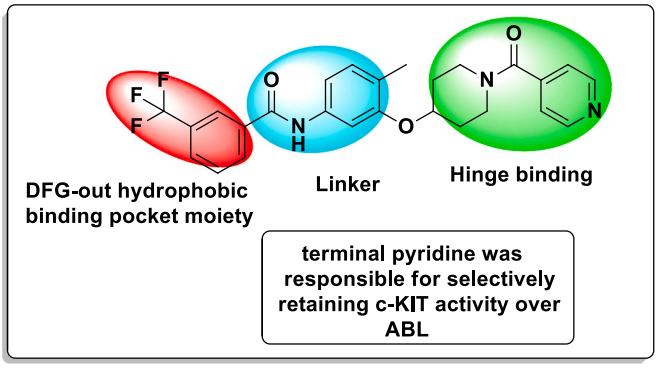

Fig. 11. The pharmacophoric description along with SAR analysis of compound **14** for c-Kit inhibitory activity.

importantly, **16** did not show any significant activity against different mutants (V654A, D816V) of c- KIT mutants [91].

In 2016, Park et al. virtually screened 40,000 natural product molecules against wild type and D816V mutant c-Kit using molecular docking analysis. Following the screening protocol, they collected the top 100 hits separately for both the targets and found that 37 molecules were common in both sets. Further, the common 37 molecules were subjected to experimental validation for their inhibitory potential against both wild-type and D816V mutant c-Kit. This protocol led to the identification of four natural product-based molecules as dual inhibitors of both wild type and D816V mutant of c-Kit (Fig. 14). Molecular docking analysis revealed that the top compounds orient themselves similarly in the ATP-binding pocket of both targets. Expectedly polar moieties on the fused aromatic ring systems form the essential H-bonds with Cys673 [93].

In 2017, Huang et al. reported the development of indolinone-based multi-kinase inhibitors for the management of idiopathic pulmonary fibrosis (IPF). In the study, a shape-based scaffold hopping approach was followed whereby they converted the amino aryl ring of nintedanib to dihydroindole nucleus, eventually resulting in compound **17**, the most potent member of the series. SAR studies suggested that the terminal morpholine ring as amine tail improved the potency (Fig. 15). In addition to c-Kit, compound **17** was also found to inhibit PDGFR and RET kinase. Further, the pharmacokinetic profile of **17** was found to be favorable for further development [94].

In 2017, Lu et al. reported lead optimization of a multi-kinase inhibitor, **18** (Linifanib), leading to the design and synthesis of 3-substituted-pyrazolo[3,4-*b*]pyridine based c-Kit/PDGFRα inhibitor,

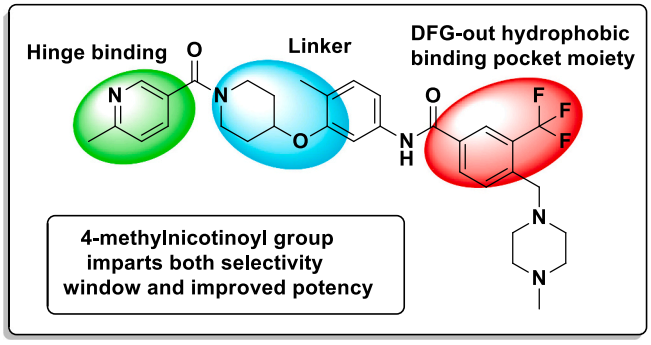

Fig. 13. The pharmacophoric description along with SAR analysis of compound **16** for c-Kit inhibitory activity.

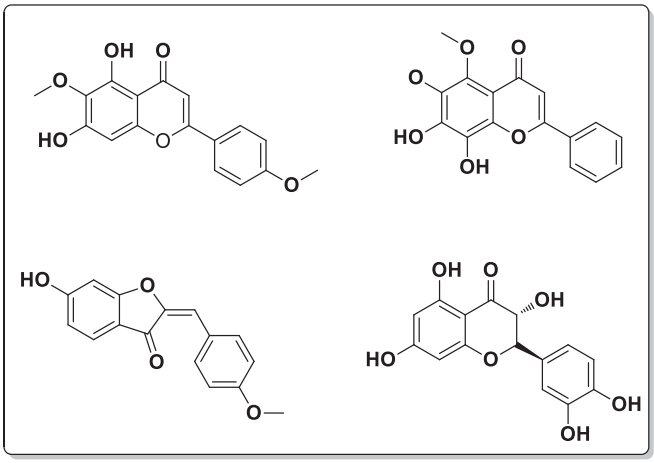

Fig. 14. 2-D structures of natural product compounds reported possessing c-Kit inhibitory activity.

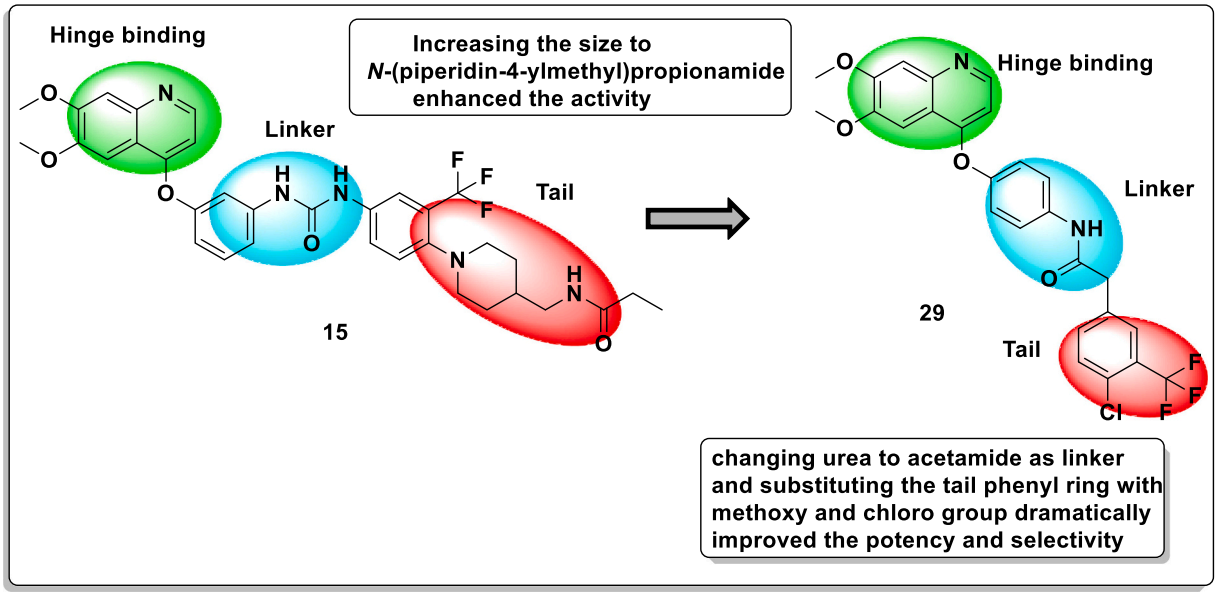

Fig. 12. The pharmacophoric description along with SAR analysis of compound **15** for c-Kit inhibitory activity.

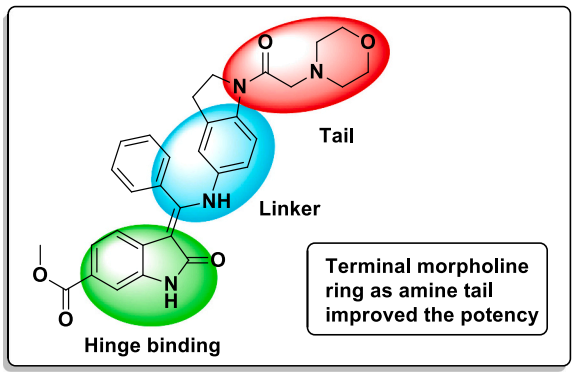

Fig. 15. The pharmacophoric description along with SAR analysis of compound **17** for c-Kit inhibitory activity.

shifting activity spectrum from VEGFR/PDGFR. SAR analysis revealed that the 3-methyl-pyrazolo[3,4-b] pyridine core is important for the c-Kit/ PDGFRα dual inhibitory activity. Additionally, the terminal amines were also found to be well correlated with the activity. Out of all, the most potent compound, **19** showed nanomolar range activity against c-Kit with an IC_{50} value of 2.4 nM (Fig. 16). Further *in-vitro* evaluation disclosed that **19** showed potency against various cancer cell lines, including GIST-882 cells, while it showed no activity against BCR-ABL driven CML cell lines. Moreover, **19** showed no toxicity against normal cell lines with almost no hERG inhibitory activity, suggesting it possesses a good safety profile [95].

In 2018, Kettle et al. reported the identification of quinazoline-based type II mutant c-Kit inhibitors. In the current work, Kettle et al. utilized the lead molecule AZD2932 (**20**), which they identified in their previous work as VEGFR-2 and PDGFR inhibitor and explored the possibility of designing a c-Kit inhibitor using its core. Incorporating different substituents led to the identification of some potent inhibitors of c-Kit. SAR analysis revealed that the presence of the fluoro group at C-5 of the core improved potency. Similarly, the presence of the methoxyethoxy group at C-7 resulted in the optimization of potency against mutant c-Kit (Fig. 17). The interaction diagram of the top compound **21** in the catalytic domain of c-Kit revealed that triazole ring occupies the DFG pocket, while the methoxyethoxy tail protrudes out of the pocket in the solvent accessible region. Upon biological evaluation, **21** showed a potent inhibitory profile with nanomolar range IC_{50} values. More importantly, in mouse allograft tumor models using these Ba/F3 lines, **21** showed potency at a dose of 20 mg/kg [96].

In 2018 Lin et al. designed and synthesized dihydrofuropyrimidine-based multi-kinase inhibitors targeting Syk, PDGFR-α, and c-Kit. SAR analysis of the synthesized compounds revealed that the presence of methoxy groups on the aryl ring coupled to amino pyrimidine core is important for the activity. Interestingly upon fusing the 3,4-methoxy group into 1,4-dioxane, the compound retained Syk and c-Kit dual inhibitory potential while lacking PDGFR-α inhibitory activity (Fig. 18). Out of all, compound **22** showed optimal inhibitory potential against all three kinases. Detailed molecular modeling studies disclosed that the carbamoylnicotinic acid group forms two H-bond interactions with Glu640 and Thr670 in the catalytic domain of c-Kit. While a critical interaction between the methoxy group on the aryl ring and Ile571 was also observed, justifying the potential of the compounds against c-Kit. In biological evaluation, compound **22** showed potent anti-proliferative potential against FLSs and mBMMCs with sub-micromolar IC_{50} values and a significant decrease in the levels of inflammatory cytokines [97].

In 2019, Wu et al. reported a series of urea-substituted thiazol-2-ylamine pyrimidine derivatives as inhibitors of c-Kit and other clinically relevant mutants of c-Kit. SAR analysis suggested that phenyl-substituted urea was a critical structural feature for c-Kit inhibitory potential. Also, it was observed that the replacement of the 5-ethylisoxazole or urea group did not alter the activity of the compounds (Fig. 19). Of all the derivatives, compound **23** exhibited high potency against c-Kit in both enzymatic assay, IC_{50} of 82 nM, and cellular assay, GI_{50} = 2.2 nM, which was also significantly better than sunitinib. Upon detailed *in-vivo* evaluation, compound **23** also induced tumor regression in the xenograft mouse model. Further co-crystallized structure of compound **23** in the catalytic domain of c-Kit revealed that it binds as a type II inhibitor. More importantly, it was also observed **23** could also switch the active conformation of c-Kit to inactive conformation. The interaction diagram of **23** indicates that the thiazolylamine core forms two H-bonds with Cys673, while the tail group forms three H-bonds with Glu640 and Asp810, occupying the back pocket of the ATP binding site [98].

In 2019, Quattrini et al. reported the design, synthesis, and evaluation of 1,2,4-triazole derivatives as c-Kit/AurB dual kinase inhibitors. The designing of these molecules included structural modifications in a previously reported hit, **24**, followed by molecular docking analysis. Docking revealed that the triazole core forms H-bond with Cys673 and 5-phenyl group makes additional hydrophobic interactions with Val603, Ala621, Lys623, Tyr672, Tyr675, Met757, and Cys809.

Out of all, compound **25** was found to possess potent anti-proliferative potential against A2058 and WM266-4 melanoma cell lines. SAR analysis revealed that the chloro group on the 5-phenyl ring

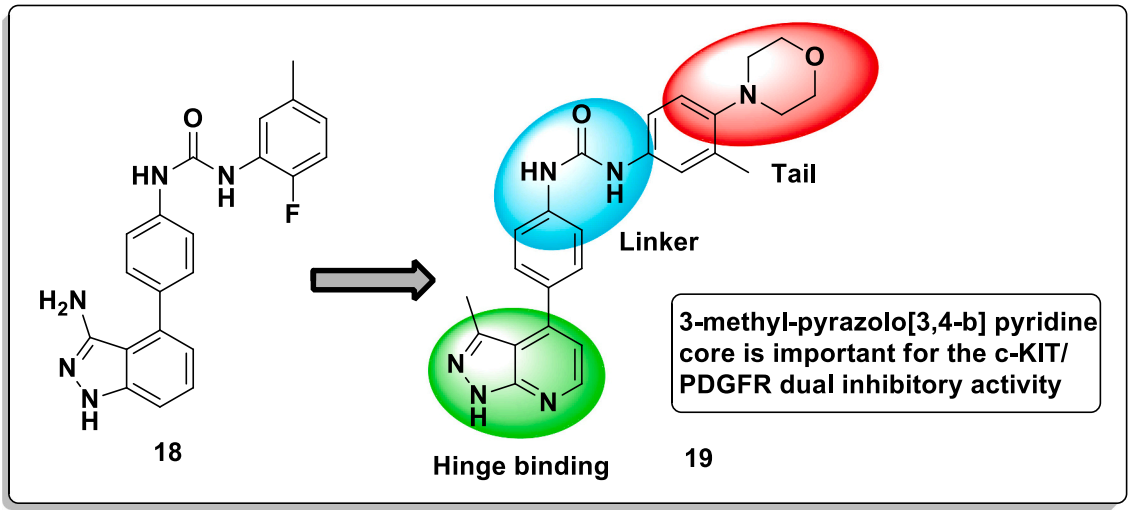

Fig. 16. The pharmacophoric description along with SAR analysis of compound **19** for c-Kit inhibitory activity.

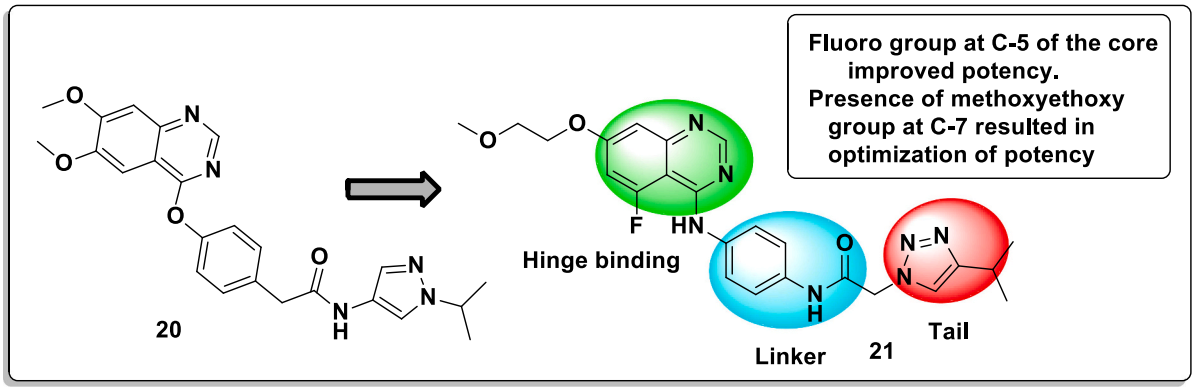

Fig. 17. The pharmacophoric description along with SAR analysis of compound **21** for c-Kit inhibitory activity.

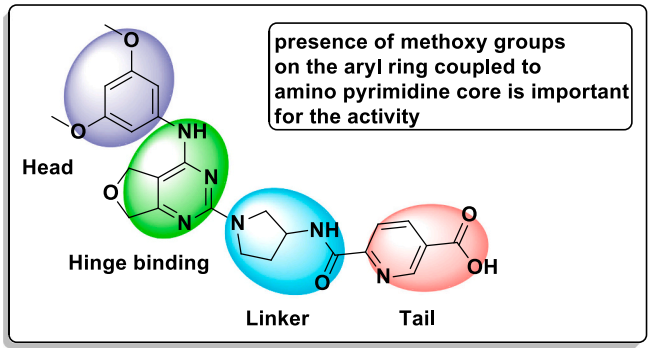

Fig. 18. The pharmacophoric description along with SAR analysis of compound **22** for c-Kit inhibitory activity.

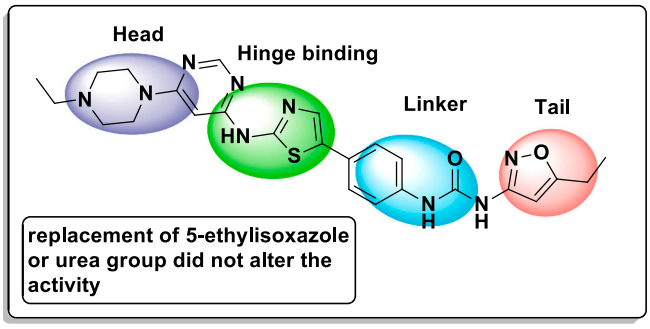

Fig. 19. The pharmacophoric description along with SAR analysis of compound **23** for c-Kit inhibitory activity.

and a 2,5-dimethoxy group on the distal phenyl ring improves the c-Kit inhibitory potential (Fig. 20) [99].

In 2019 Liu et al. optimized an already known multi-kinase inhibitor **26** with moderate inhibitory potential against wild type and mutant variants of c-Kit. They followed a hybrid fragment-based drug design approach and identified indazole-based inhibitors of c-Kit, with selectivity against T670I mutant. Interestingly, the most potent compound **27** showed a Type-II binding mode while the lead molecule, **26,** can bind both as Type-I and II inhibitors. SAR analysis revealed that using malonamide moiety as a linker improved the potency while substituting meta-halogen-substituted phenyl rings as a tail group resulted in the most potent compound (Fig. 21). Importantly using bulky hydrophobic groups instead of halogens reduced the activity. Binding mode analysis of the top compound, **27,** showed that the indazol core forms two H-bond interactions with Cys673 and Glu671. More importantly, in the binding site of T670I mutant c-Kit, the malonamide linker provides enough room to accommodate Ile670, imparting the selectivity. Further biochemical assay results indicated that compound **27** showed 10 − 30-fold selectivity for T670I mutant c-Kit over wild type c-Kit. Additionally, it also exhibited a significant anti-proliferative effect against both imatinib-sensitive and imatinib-resistant cell lines [100].

In 2019, Sun et al. reported the utilization of 2,7-naphthyridone scaffold for the design and synthesis of 8-amino-substituted 2-phenyl-2,7- naphthyridin-1(2H)-one derivatives as dual inhibitors of c-Kit and VEGFR2. A small library of derivatives was synthesized and evaluated for their kinase inhibitory potential, revealing that few compounds showed potent c-Kit and VEGFR-2 kinase inhibitory activity. Out of all, compound **28** showed a nanomolar range inhibitory effect against c-Kit (Fig. 22). Further, molecular docking analysis revealed that **28** forms H-bond interactions with Asp810 and Cys673, along with ion–π interaction with Lys623 [101].

In 2019 Wu et al. continued their previous efforts, utilized a hybrid design approach to further optimize **15,** and reported the identification of more potent c-Kit inhibitor **29**. They primarily focused on modifying the linker and tail region of **15** to improve potency and pharmacokinetic profile, which led to the synthesis of a library of compounds. SAR analysis revealed that changing urea to acetamide as a linker and substituting the tail phenyl ring with methoxy and chloro group dramatically improved the potency and selectivity (Fig. 12). Out of all, compound **29** was found to possess the most significant potency against both wild-type c-Kit (GI_{50} = 0.001 μM) and T670I mutant c-Kit (GI_{50} = 0.004 μM). Binding mode analysis of **29** disclosed that it retained a type-II binding mode with an H-bond interaction with Cys673. Also the amide linker formed two H-bond interactions with Asp810 and Glu640, with the "tail" ring occupying a hydrophobic pocket. Furthermore, the KINOMEscan results and other biological experiments indicated a good selectivity profile and inhibitory activity only against type III kinases such as CSF1R and PDGFRα/β kinases [102].

In 2019 Lin et al. employed structure-based drug designing on 5-phenylthiazol-2-ylamine as a versatile template for developing multi-kinase inhibitors, resulting in the discovery of compound **30** having potent inhibitory potential against mutant c-Kits. In this work, they synthesized a library of 5-aromatic substituted thiazol- 2-ylamine pyrimidine derivatives with modifications in the linker and tail region. Out of all, **30** possessed the most potent inhibitory profile with nanomolar range activity against GIST-T1 (GI_{50} = 7.1 nM). SAR analysis revealed that substituting pyridine with its fourth position to thiazole resulted in the most potent compound (Fig. 23). Co-crystallized structure of **30** with c-Kit disclosed that thiazol-2-ylamine core forms two H-bond interactions with Cys673, along with the hydrophobic interactions with Leu595, Tyr672, Cys673, and Leu799. Also, the pyridine ring forms an H-bond with Lys623, occupying the back pocket of the ATP-binding site. Detailed biological validation suggested that **30** possess superior efficacy and tolerability in GIST and AML tumor xenograft models [103].

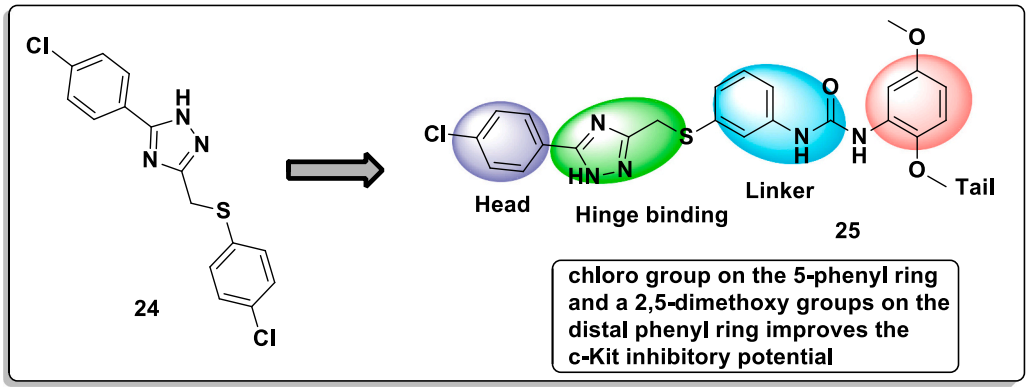

Fig. 20. The pharmacophoric description along with SAR analysis of compound **25** for c-Kit inhibitory activity.

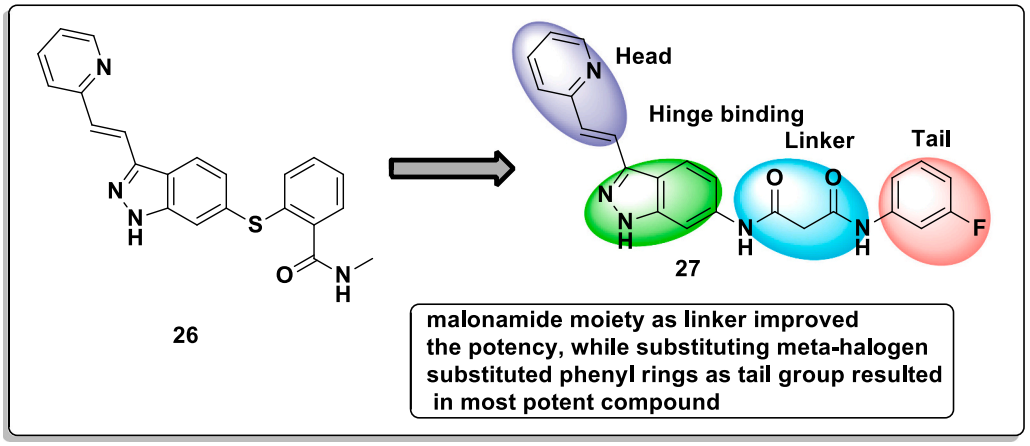

Fig. 21. The pharmacophoric description along with SAR analysis of compound **27** for c-Kit inhibitory activity.

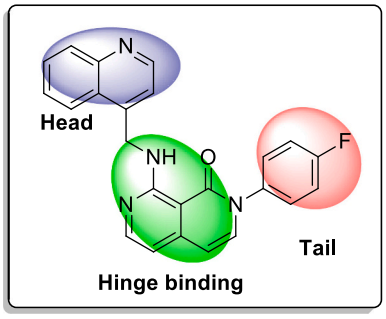

Fig. 22. Pharmacophoric description of compound **28** for c-Kit inhibitory activity.

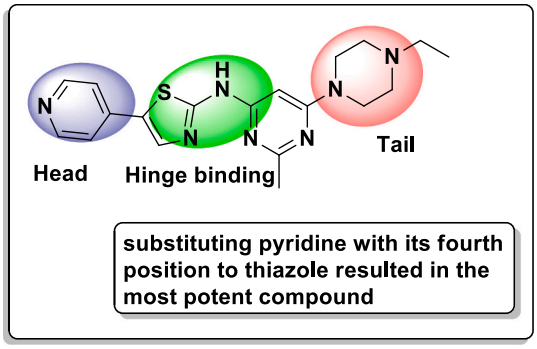

Fig. 23. The pharmacophoric description along with SAR analysis of compound **30** for c-Kit inhibitory activity.

In 2020, Martorana and Lauria performed an *in-silico* study following mixed ligand- and structure-based drug designing approaches to screen putative inhibitors of mutant c-Kit, which can overcome acquired resistance in the clinical treatment of cancer. In the study, they analyzed the binding affinity of various kinases inhibitors in the different mutants (T670I and V654A) of c-Kit. Results showed that sunitinib also exhibits good binding affinity for mutant variants of c-Kit. Further, they followed a virtual screening protocol to screen compounds against mutant variants of c-Kit. For the ligand-based drug designing approach, they employed web-server DRUDIT, which employs a comparison of molecular descriptors of molecules with the template of the receptor—followed by molecular docking analysis as a tool of structure-based drug design, which led to the identification of structures with a significant binding affinity comparable to standard inhibitors. Overall, this screening protocol yielded compounds **31**, **32**, **33**, and **34** having significant binding affinity for T670I mutant c-Kit and compounds **35** and **36** with significant binding affinity for V654A mutant c-Kit (Fig. 24) [104].

In 2021, Roy et al. synthesized and evaluated fisetin analogs as antiproliferative agents for the management of melanoma. Preliminary screening *via* MTT assay identified eleven molecules to possess better potency than fisetin. In the next step, they employed an inverse docking protocol to identify the putative molecular targets for these antiproliferative agents, which led to the selection of c-Kit, CDK2, and mTOR as probable targets. Expectedly, most of the compounds were

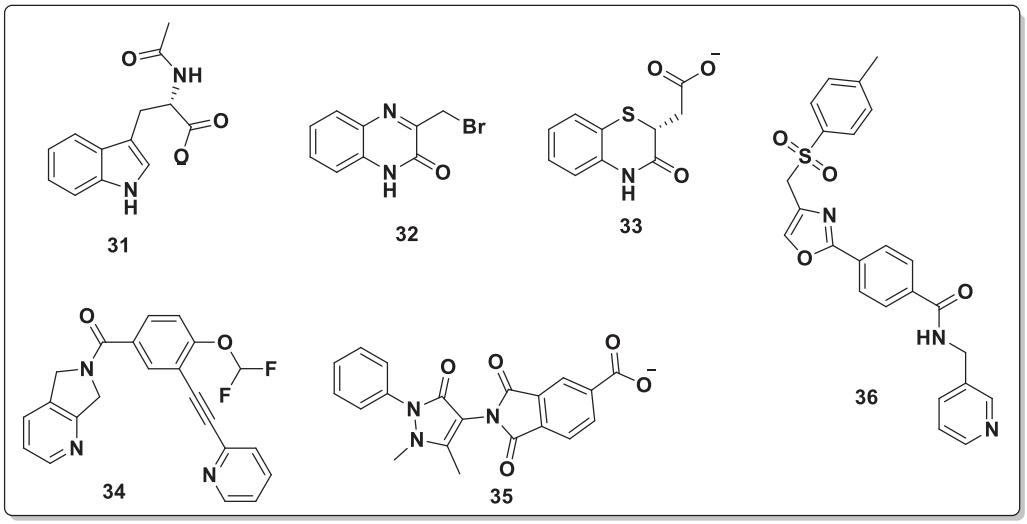

Fig. 24. 2-D structures of screened hits reported with c-Kit inhibitory activity.

reported to form H-bond interactions with Cys673 in the catalytic domain of c-Kit. Further, the compounds were evaluated for their inhibitory potential against the selected kinases. Interestingly, almost all the eleven compounds were found to be the potent inhibitors of c-Kit with sub-micromolar range IC_{50}, in comparison to CDK2 and mTOR. Out of all, compound **37** was found to possess better potency against c-Kit, with a better anti-proliferative profile in wound healing and other biological experiments. Limited SAR suggested that the presence of electron-withdrawing groups improved the activity against c-Kit (Fig. 25). The obtained data indicated that the synthesized analogs, lacking the 7-hydroxy group on ring A, were having improved anti-proliferative/ cytotoxic properties [105,106].

7. FDA-approved drugs targeting c-Kit

There are a few small-molecule heterocycles approved by the FDA as c-Kit inhibitors for the management of different types of cancer (Table 4). Expectedly, FDA-approved molecules also highlight similar structural features like most preclinical candidates, fulfilling the pharmacophoric requirements for c-Kit inhibition.

8. How to design c-Kit inhibitors: crucial structural features needed for inhibition

By carefully investigating all the small molecule heterocycles reported as c-Kit inhibitors, some generalizations can be made. As pointed above, it can be seen that most of the c-Kit inhibitors are multi-targeting, and although there are some advantages of multi-target kinases inhibitors in certain types of cancer, few researchers have attempted, or succeeded, to develop selective c-Kit for cancer subtypes, which are highly dependent on activating mutations in c-Kit. Here, we will discuss the basics of chemical modifications and structural features needed to design potent and selective c-Kit inhibitors. One of the most important

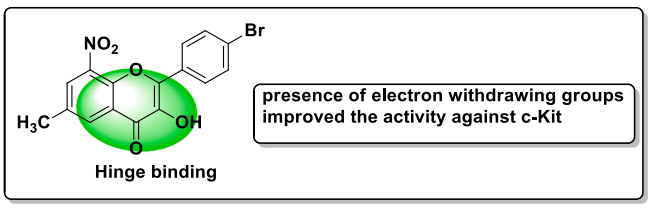

Fig. 25. The pharmacophoric description along with SAR analysis of compound **37** for c-Kit inhibitory activity.

requirements for c-Kit inhibition is that the heterocycle core, which occupies the hinge binding domain, should maintain a bidentate H-bonding interaction with Cys673. The strength and stability of this bidentate interaction with Cys673 serves as a critical factor for the potency and selectivity of the c-Kit inhibitor. Therefore, it can be observed that almost all the selective c-Kit inhibitors use a bicyclic nitrogen-based heterocycle as the core for the hinge binding domain. The second set of crucial interactions includes two typical H-bond interactions formed between the linker, usually an amide moiety, and Glu640 in the c-helix and Asp810 of the DFG motif. This interaction also strengthens the H-bond with Cys673. Finally, the DFG out conformation generates a hydrophobic pocket occupied by the tail of the molecules. As evident from the discussion in section 6, molecules with tri-methoxy substituted aryl ring or halogen-substituted aryl rings as tail have higher affinity against c-Kit. Analysis of four c-Kit inhibitors (**9**, **21**, **22,** and **29**) also validated the same. Compounds **9** and **29** maintained all the three crucial interactions (H-bond of the heterocyclic core with Cys673, H-bond between linker and Asp810, and lastly tail occupying the hydrophobic pocket), leading to selective and potent c-Kit inhibition. In contrast, on the other hand, compounds 21 and 22 do not fulfill all the required conditions and are not so selective c-Kit inhibitors (Fig. 26). Therefore, molecules with structural features to maintain the aforementioned interactions have been reported to show selective and potent c-Kit inhibition.

9. Conclusion

c-Kit and its physiological functions were first elucidated roughly two decades ago. Since then, there have been significant advances in the knowledge concerning its implications in both normal and disease-state cellular functions. As a type-III receptor tyrosine kinase, it is involved in several signaling pathways, including the PI3K pathway, MAPK pathway, *etc.*, responsible for cellular growth and proliferation. In medicinal chemistry and drug discovery, c-Kit is considered one of the key targets for the management of various types of cancer, including melanoma and GISTs. Structurally, it contains three domains: (a) a hydrophobic transmembrane, (b) an extracellular ligand-binding domain, and (c) a tyrosine kinase activity domain in the cytoplasm. Similarly to other tyrosine kinases, c-Kit, and its ATP-binding pocket have been extensively explored as a possible target for anti-cancer drugs. Almost all the medicinal chemistry groups working on c-Kit have been designing ATP-competitive inhibitors. A general conclusion could be made that almost all the c-Kit inhibitors possess four sub-structural/pharmacophoric features: (1) a nitrogen heterocycle as head, (2) hinge binding feature, (3) a

Table 4
List of FDA-approved inhibitors along with the pharmacophoric features.

Compound	Structure	Head	Hinge binding	Linker	Tail
Sorafenib	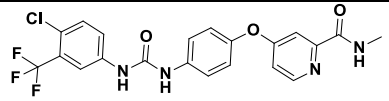		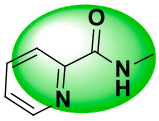	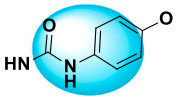	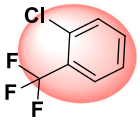
Imatinib	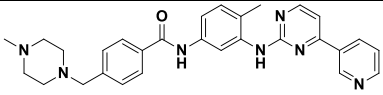	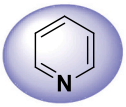		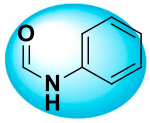	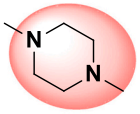
Dasatinib	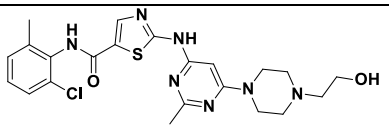		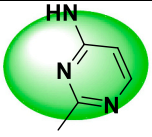	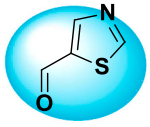	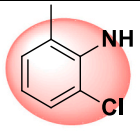
Sunitinib	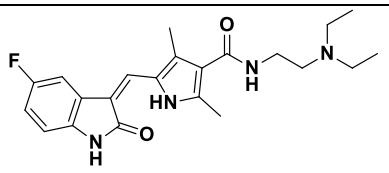		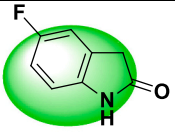	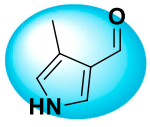	
Nilotinib	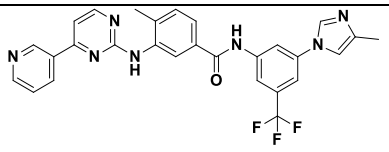	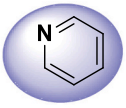	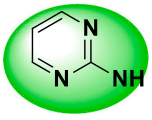	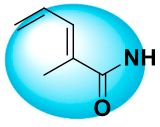	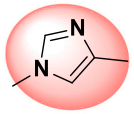
Amuvatinib	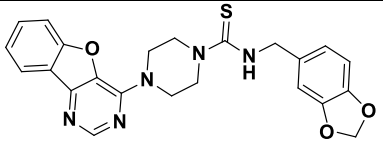		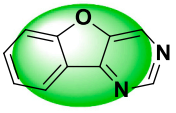		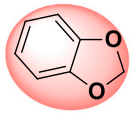
Regorafenib	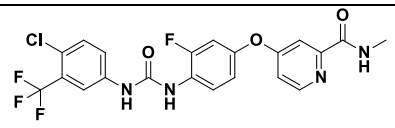		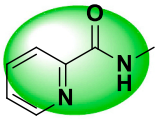	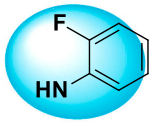	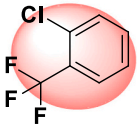
Avapritinib	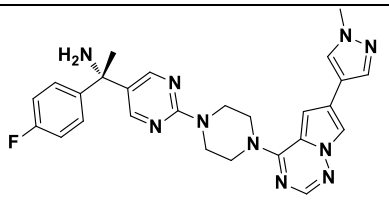	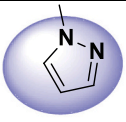	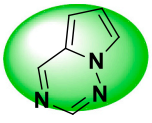	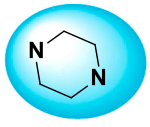	
Ripretinib	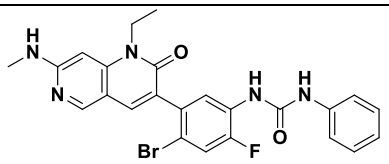		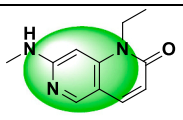	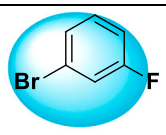	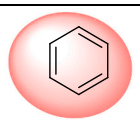
Tivozanib	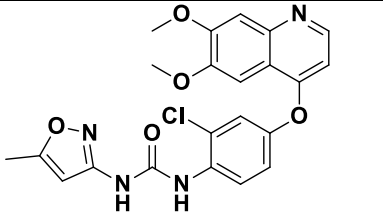				

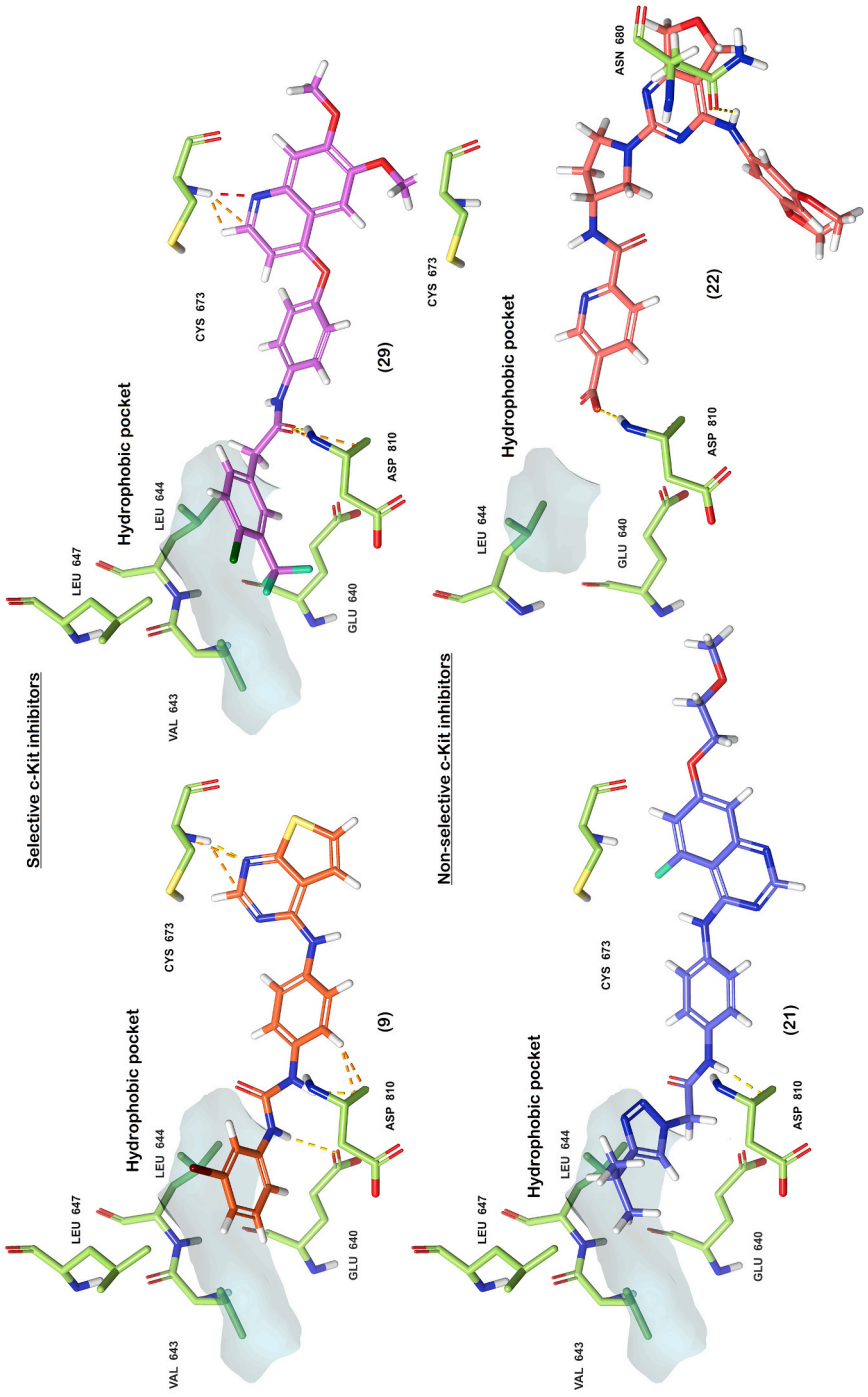

Fig. 26. Comparative analysis of different selective and non-selective c-Kit inhibitors.

linker, and (4) a tail ring. These four features have been widely explored by using slightly modified substituents to understand and manipulate the selectivity and potency of the inhibitors. Also, the modifications of linker-region to alter the flexibility of the compounds have been noticed to affect the selectivity amongst different mutant isoforms of c-Kit. However, there are no compilations providing reflections on the design, SAR, and inhibition of c-Kit. As such, the observations and findings provided in this compilation provide much-needed information about the structure, signaling, and inhibitors of c-Kit. In the future, these data could be utilized in c-Kit-targeted anti-cancer drug discovery.

Declaration of Competing Interest

Authors have no conflict of interest.

Acknowledgment

PKS would like to thank TCSMT for the Postdoctoral fellowship.

References

[1] P.K. Singh, H. Singh, O. Silakari, Kinases inhibitors in lung cancer: from benchside to bedside, Biochim.Biophys.Acta 1866 (2016) 128–140.
[2] K.S. Bhullar N.O. Lagarón E.M. McGowan I. Parmar A. Jha B.P. Hubbard H.V. Rupasinghe Kinase-targeted cancer therapies: progress, challenges and future directions Mol.Cancer 17 2018 1 20.
[3] P. Singh, O. Silakari, Molecular dynamics and pharmacophore modelling studies of different subtype (ALK and EGFR (T790M)) inhibitors in NSCLCSAR QSAR 28 (2017) 221–233.
[4] P.K. Singh, O. Silakari, Novel EGFR (T790M)-cMET dual inhibitors: putative therapeutic agents for non-small-cell lung cancer, Future Med.Chem. 9 (2017) 469–483.
[5] P.K. Singh, O. Silakari, Molecular dynamics guided development of indole based dual inhibitors of EGFR (T790M) and c-MET, Bioorg.Chem. 79 (2018) 163–170.
[6] P.K. Singh, D. Chaudhari, S. Jain, O. Silakari, Structure based designing of triazolopyrimidone-based reversible inhibitors for kinases involved in NSCLC, Bioorg.Med.Chem.Lett. 29 (2019) 1565–1571.
[7] P. Kumar Singh, O. Silakari, In silico guided development of imine-based inhibitors for resistance-deriving kinases, J.Biomol.Struct.Dyn. 37 (2019) 2593–2599.
[8] C.E. Edling, B. Hallberg, C-Kit—a hematopoietic cell essential receptor tyrosine kinase, Int.J.Biochem.CellBiol. 39 (2007) 1995–1998.
[9] A.F. Abdel-Magid The Potential of c-KIT KinaseInhibitors in CancerTreatment ACS Publications 2021.
[10] B. Wehrle-Haller, The role of kit-ligand in melanocyte development and epidermal homeostasis, Pigment CellRes. 16 (2003) 287–296.
[11] J. Lennartsson, L. Rönnstrand, Stem cell factor receptor/c-kit: from basic science to clinical implications, Physiol.Rev. 92 (2012) 1619–1649.
[12] B. Phung, J. Sun, A. Schepsky, E. Steingrimsson, L. Rönnstrand, C-KIT signaling depends on microphthalmia-associated transcription factor for effects on cell proliferation, PLoS One 6 (2011), e24064.
[13] K.T. Montone P. Van Belle R. Elenitsas D.E. Elder, Proto-oncogene c-kit expression in malignant melanoma: protein loss with tumor progression, Modern Pathol.10 (1997) 939–944.
[14] Y. Isabel Zhu, J.E. Fitzpatrick, Expression of c-kit (CD117) in spitz nevus and malignant melanoma, J.Cutan.Pathol. 33 (2006) 33–37.
[15] A. Slipicevic, M. Herlyn, KIT in melanoma: many shades of gray, J.Investig. Dermatol. 135 (2015) 337–338.
[16] S. Huang, M. Luca, M. Gutman, D.J. McConkey, K.E. Langley, S.D. Lyman, M. Bar-Eli, Enforced c-KIT expression renders highly metastatic human melanoma cells susceptible to stem cell factor-induced apoptosis and inhibits their tumorigenic and metastatic potential, Oncogene 13 (1996) 2339–2347.
[17] S. Hirota, K. Isozaki, Y. Moriyama, K. Hashimoto, T. Nishida, S. Ishiguro, K. Kawano, M. Hanada, A. Kurata, M. Takeda, Gain-of-function mutations of c-kit in human gastrointestinal stromal tumors, Science 279 (1998) 577–580.
[18] S. Hirota, K. Isozaki, Pathology of gastrointestinal stromal tumors, Pathol.Int. 56 (2006) 1–9.
[19] H. Ikeda Y. Kanakura T. Tamaki A. Kuriu H. Kitayama J. Ishikawa Y. Kanayama T. Yonezawa S. Tarui J.D. Griffin, Expression and Functional Role of the Proto-oncogene c-kit in Acute Myeloblastic Leukemia Cells, (1991).
[20] M. Malaise, D. Steinbach, S. Corbacioglu, Clinical implications of c-kit mutations in acute myelogenous leukemia, Curr.Hematol.Malign.Rep. 4 (2009) 77–82.
[21] C.E. Hoei-Hansen, S.M. Kraggerud, V.M. Abeler, J. Kærn, E. Rajpert-De Meyts, R. A. Lothe, Ovarian dysgerminomas are characterised by frequent KIT mutations and abundant expression of pluripotency markers, Mol. Cancer 6 (2007) 1–12.
[22] N.M. Kamal, U. Khan, S. Mirza, K. Mazoun, F.M. Mirza, M. Jundi, Ovarian dysgerminoma with normal serum tumour markers presenting in a child with precocious puberty, J.CancerRes.Ther. 11 (2015) 661.
[23] R.S. Rivera, H. Nagatsuka, M. Gunduz, B. Cengiz, E. Gunduz, C.H. Siar, H. Tsujigiwa, R. Tamamura, K.N. Han, N. Nagai, C-kit protein expression correlated with activating mutations in KIT gene in oral mucosal melanoma, Virchows Arch. 452 (2008) 27–32.
[24] T.M. Wilson, I. Maric, O. Simakova, Y. Bai, E.C. Chan, N. Olivares, M. Carter, D. Maric, J. Robyn, D.D. Metcalfe, Clonal analysis of NRAS activating mutations in KIT-D816V systemic mastocytosis, Haematologica 96 (2011) 459.
[25] C. Serrano, S. George, C. Valverde, D. Olivares, A. García-Valverde, C. Suárez, R. Morales-Barrera, J. Carles, Novel insights into the treatment of imatinib-resistant gastrointestinal stromal tumors, Target.Oncol. 12 (2017) 277–288.
[26] G.D. Demetri, Targeting c-kit mutations in solid tumors: scientific rationale and novel therapeutic options, in: Seminars in Oncology, Elsevier, 2001, pp. 19–26.
[27] E. Wardelmann, S. Merkelbach-Bruse, K. Pauls, N. Thomas, H.-U. Schildhaus, T. Heinicke, N. Speidel, T. Pietsch, R. Buettner, D. Pink, Polyclonal evolution of multiple secondary KIT mutations in gastrointestinal stromal tumors under treatment with imatinib mesylate, Clin. Cancer Res. 12 (2006) 1743–1749.
[28] A. Lammie, M. Drobnjak, W. Gerald, A. Saad, R. Cote, C. Cordon-Cardo, Expression of c-kit and kit ligand proteins in normal human tissues, J.Histochem. Cytochem. 42 (1994) 1417–1425.
[29] K. Stankov, S. Popovic, M. Mikov, C-KIT signaling in cancer treatment, Curr. Pharm.Des. 20 (2014) 2849–2880.
[30] B. Chabot, D.A. Stephenson, V.M. Chapman, P. Besmer, A. Bernstein, The proto-oncogene c-kit encoding a transmembrane tyrosine kinase receptor maps to the mouse W locus, Nature 335 (1988) 88–89.
[31] M.L. Lux, B.P. Rubin, T.L. Biase, C.-J. Chen, T. Maclure, G. Demetri, S. Xiao, S. Singer, C.D. Fletcher, J.A. Fletcher, KIT extracellular and kinase domain mutations in gastrointestinal stromal tumors, Am.J.Pathol. 156 (2000) 791–795.
[32] S.R. Hubbard, Structures of serine/threonine and tyrosine kinases, in: Handbook of Cell Signaling, Elsevier, 2010, pp. 413–417. Place Published.
[33] G. Caruana, A.C. Cambareri, L.K. Ashman, Isoforms of c-KIT differ in activation of signalling pathways and transformation of NIH3T3 fibroblasts, Oncogene 18 (1999) 5573–5581.
[34] D.L. Cadena, G.N. Gill, Receptor tyrosine kinases, FASEB J. 6 (1992) 2332–2337.
[35] P.M. Chan, S. Ilangumaran, J. La Rose, A. Chakrabartty, R. Rottapel, Autoinhibition of the kit receptor tyrosine kinase by the cytosolic juxtamembrane region, Mol.Cell.Biol. 23 (2003) 3067–3078.
[36] C.D. Mol, K.B. Lim, V. Sridhar, H. Zou, E.Y. Chien, B.-C. Sang, J. Nowakowski, D. B. Kassel, C.N. Cronin, D.E. McRee, Structure of a c-kit product complex reveals the basis for kinase transactivation, J.Biol.Chem. 278 (2003) 31461–31464.
[37] P. Wollberg, J. Lennartsson, E. Gottfridsson, A. Yoshimura, L. Rönnstrand, The adapter protein APS associates with the multifunctional docking sites Tyr-568 and Tyr-936 in c-kit, Biochem.J. 370 (2003) 1033–1038.
[38] S. Agarwal, J.U. Kazi, S. Mohlin, S. Påhlman, L. Rönnstrand, The activation loop tyrosine 823 is essential for the transforming capacity of the c-kit oncogenic mutant D816V, Oncogene 34 (2015) 4581–4590.
[39] J.P. DiNitto, G.D. Deshmukh, Y. Zhang, S.L. Jacques, R. Coli, J.W. Worrall, W. Diehl, J.M. English, J.C. Wu, Function of activation loop tyrosine phosphorylation in the mechanism of c-Kit auto-activation and its implication in sunitinib resistance, J.Biochem. 147 (2010) 601–609.
[40] S. Sartini, B. Dario, M. Morelli, F. Da Settimo, C. La Motta, Receptor tyrosine kinase kit and gastrointestinal stromal tumours: an overview, Curr.Med.Chem. 18 (2011) 2893–2903.
[41] B. Heissig, Z. Werb, S. Rafii, K. Hattori, Role of c-kit/Kit ligand signaling in regulating vasculogenesis, Thromb.Haemost. 90 (2003) 570–576.
[42] A.L. Smith, F.M. Ellison, J.P. McCoy Jr., J. Chen, C-kit expression and stem cell factor-induced hematopoietic cell proliferation are up-regulated in aged B6D2F1 mice, J.Gerontol.Ser.ABiol.Sci.Med.Sci. 60 (2005) 448–456.
[43] J.Y. Shin, W. Hu, M. Naramura, C.Y. Park, High c-kit expression identifies hematopoietic stem cells with impaired self-renewal and megakaryocytic bias, J. Exp.Med. 211 (2014) 217–231.
[44] F. Colucci, J.P.Di Santo, The receptor tyrosine kinase c-kit provides a critical signal for survival, expansion, and maturation of mouse natural killer cells, Blood 95 (2000) 984–991.
[45] B.N. Vajravelu, K.U. Hong, T. Al-Maqtari, P. Cao, M.C. Keith, M. Wysoczynski, J. Zhao, J.B. Moore IV, R. Bolli, C-kit promotes growth and migration of human cardiac progenitor cells via the PI3K-AKT and MEK-ERK pathways, PLoS One 10 (2015), e0140798.
[46] H.J. Cardoso, M.I. Figueira, S. Correia, C.V. Vaz, S. Socorro, The SCF/c-KIT system in the male: survival strategies in fertility and cancer, Mol.Reprod.Dev. 81 (2014) 1064–1079.
[47] V. Alexeev, K. Yoon, Distinctive role of the cKit receptor tyrosine kinase signaling in mammalian melanocytes, J.Investig.Dermatol. 126 (2006) 1102–1110.
[48] M.A. Pezzone, S.C. Watkins, S.M. Alber, W.E. King, W.C. de Groat, M. B. Chancellor, M.O. Fraser, americanjournal of physiology-renalPhysiology 284 (2003) F925–F929.
[49] K. Bantubungi, D. Blum, L. Cuvelier, S. Wislet-Gendebien, B. Rogister, E. Brouillet, S.N. Schiffmann, Stem cell factor and mesenchymal and neural stem cell transplantation in a rat model of Huntington's disease, Mol.Cell.Neurosci. 37 (2008) 454–470.
[50] P. Nigro, G.L. Perrucci, A. Gowran, M. Zanobini, M.C. Capogrossi, G. Pompilio, C-kit+ cells: the tell-tale heart of cardiac regeneration? Cell.Mol. Life Sci. 72 (2015) 1725–1740.
[51] I. Aquila, E. Cianflone, M. Scalise, F. Marino, T. Mancuso, A. Filardo, A.J. Smith, D. Cappetta, A. De Angelis, K. Urbanek, C-kithaploinsufficiency impairs adult cardiac stem cell growth, myogenicity and myocardial regeneration, Cell DeathDis. 10 (2019) 1–19.

[52] F. Marino, M. Scalise, E. Cianflone, T. Mancuso, I. Aquila, V. Agosti, M. Torella, D. Paolino, V. Mollace, B. Nadal-Ginard, Role of c-kit in myocardial regeneration and aging, Front.Endocrinol. 10 (2019) 371.
[53] R. Kerkelä, L. Grazette, R. Yacobi, C. Iliescu, R. Patten, C. Beahm, B. Walters, S. Shevtsov, S. Pesant, F.J. Clubb, Cardiotoxicity of the cancer therapeutic agent imatinib mesylate, Nat.Med. 12 (2006) 908–916.
[54] H.J. Cardoso, M.I. Figueira, S. Socorro, The stem cell factor (SCF)/c-KIT signalling in testis and prostate cancer, J.Cell Commun.Signal. 11 (2017) 297–307.
[55] K. Liu, Stem cell factor (SCF)-kit mediated phosphatidylinositol 3 (PI3) kinase signaling during mammalian oocyte growth and early follicular development, Front. Biosci. 11 (2006) 126–135.
[56] A. Yasuda, H. Sawai, H. Takahashi, N. Ochi, Y. Matsuo, H. Funahashi, M. Sato, Y. Okada, H. Takeyama, T. Manabe, Stem cell factor/c-kit receptor signaling enhances the proliferation and invasion of colorectal cancer cells through the PI3K/Akt pathway, Dig.Dis.Sci. 52 (2007) 2292–2300.
[57] E. Wandzioch, C.E. Edling, R.H. Palmer, L. Carlsson, B. Hallberg, Activation of the MAP kinase pathway by c-kit is PI-3 kinase dependent in hematopoietic progenitor/stem cell lines, Blood 104 (2004) 51–57.
[58] J. Lennartsson, P. Blume-Jensen, M. Hermanson, E. Pontén, M. Carlberg, L. RoÈnnstrand, Phosphorylation of shc by src family kinases is necessary for stem cell factor receptor/c-kit mediated activation of the Ras/MAP kinase pathway and c-fos induction, Oncogene 18 (1999) 5546–5553.
[59] K.S. Smalley, V.K. Sondak, J.S. Weber, c-KIT signaling as the driving oncogenic event in sub-groups of melanomas, Histol.Histopathol. 24 (2009) 643–650.
[60] S. Pathania, R.K. Rawal, An update on chemical classes targeting ERK1/2 for the management of cancer, Future Med.Chem. 12 (2020) 593–611.
[61] S. Pathania, P.K. Singh, R.K. Narang, R.K. Rawal, Identifying novel putative ERK1/2 inhibitors via hybrid scaffold hopping–FBDD approach, J.Biomol.Struct. Dyn. (2021) 1–16.
[62] O. Voytyuk, J. Lennartsson, A. Mogi, G. Caruana, S. Courtneidge, L.K. Ashman, L. Ronnstrand, Src family kinases are involved in the differential signaling from two splice forms of c-kit, J.Biol.Chem. 278 (2003) 9159–9166.
[63] V.C. Broudy, N.L. Lin, W.C. Liles, S.J. Corey, B. O'Laughlin, S. Mou, D. Linnekin 94 (1999) 1979–1986.
[64] G. Cruse, D.D. Metcalfe, A. Olivera, Functional deregulation of KIT: link to mast cell proliferative diseases and other neoplasms, Immunol.Allergy Clin. 34 (2014) 219–237.
[65] D. Linnekin, S. Mou, C.S. Deberry, S.R. Weiler, J.R. Keller, F.W. Ruscetti, D. L. Longo, Stem cell factor, the JAK-STAT pathway and signal transduction, Leukemia Lymphoma 27 (1997) 439–444.
[66] J. Bromberg, Stat proteins and oncogenesis, J.Clin.Invest. 109 (2002) 1139–1142.
[67] L.K. Ashman, R. Griffith, Therapeutic targeting of c-KIT in cancer, Expert Opin. Investig.Drugs 22 (2013) 103–115.
[68] C. Willmore-Payne, J.A. Holden, S. Hirschowitz, L.J. Layfield, BRAF and c-kit gene copy number in mutation-positive malignant melanoma, Hum.Pathol. 37 (2006) 520–527.
[69] S. Tsutsui, K. Yasuda, K. Suzuki, H. Takeuchi, T. Nishizaki, H. Higashi, S. Era, A loss of c-kit expression is associated with an advanced stage and poor prognosis in breast cancer, Br.J.Cancer 94 (2006) 1874–1878.
[70] S.E. Woodman, J.C. Trent, K. Stemke-Hale, A.J. Lazar, S. Pricl, G.M. Pavan, M. Fermeglia, Y.V. Gopal, D. Yang, D.A. Podoloff, Activity of dasatinib against L576P KIT mutant melanoma: molecular, cellular, and clinical correlates, Mol. CancerTher. 8 (2009) 2079–2085.
[71] C. Bodemer, O. Hermine, F. Palmérini, Y. Yang, C. Grandpeix-Guyodo, P. S. Leventhal, S. Hadj-Rabia, L. Nasca, S. Georgin-Lavialle, A. Cohen-Akenine, Pediatric mastocytosis is a clonal disease associated with D816V and other activating c-KIT mutations, J.Investig.Dermatol. 130 (2010) 804–815.
[72] J. Pan, A. Quintás-Cardama, H.M. Kantarjian, C. Akin, T. Manshouri, P. Lamb, J. E. Cortes, A. Tefferi, F.J. Giles, S. Verstovsek, EXEL-0862, a novel tyrosine kinase inhibitor, induces apoptosis in vitro and ex vivo in human mast cells expressing the KIT D816V mutation, Blood 109 (2007) 315–322.
[73] T. Kajiguchi, S. Lee, M.-J. Lee, J.B. Trepel, L. Neckers, KIT regulates tyrosine phosphorylation and nuclear localization of β-catenin in mast cell leukemia, Leuk. Res. 32 (2008) 761–770.
[74] M.A. Babaei, B. Kamalidehghan, M. Saleem, H.Z. Huri, F. Ahmadipour, Receptor tyrosine kinase (c-Kit) inhibitors: a potential therapeutic target in cancer cells, Drug Des.Dev.Ther. 10 (2016) 2443.
[75] F. Broekman, E. Giovannetti, G.J. Peters, Tyrosine kinase inhibitors: multi-targeted or single-targeted? World J.Clin.Oncol. 2 (2011) 80.
[76] A.J. Garton, A.P. Crew, M. Franklin, A.R. Cooke, G.M. Wynne, L. Castaldo, J. Kahler, S.L. Winski, A. Franks, E.N. Brown, OSI-930: a novel selective inhibitor of kit and kinase insert domain receptor tyrosine kinases with antitumor activity in mouse xenograft models, Cancer Res. 66 (2006) 1015–1024.
[77] J.P. Patel, Y.-H. Kuang, Z.-S. Chen, V.L. Korlipara, Inhibition of c-kit, VEGFR-2 (KDR), and ABCG2 by analogues of OSI-930, Bioorg.Med.Chem.Lett. 21 (2011) 6495–6499.
[78] R.J. Davies, A.C. Pierce, C. Forster, R. Grey, J. Xu, M. Arnost, D. Choquette, V. Galullo, S.-K. Tian, G. Henkel, Design, synthesis, and evaluation of a novel dual FMS-like tyrosine kinase 3/stem cell factor receptor (FLT3/c-KIT) inhibitor for the treatment of acute myelogenous leukemia, J.Med.Chem. 54 (2011) 7184–7192.
[79] D.K. Heidary, G. Huang, D. Boucher, J. Ma, C. Forster, R. Grey, J. Xu, M. Arnost, D. Choquette, G. Chen, VX-322: a novel dual receptor tyrosine kinase inhibitor for the treatment of acute myelogenous leukemia, J.Med.Chem. 55 (2012) 725–734.
[80] A.M. Almerico, M. Tutone, A. Lauria, Receptor-guided 3D-QSAR approach for the discovery of c-kit tyrosine kinase inhibitors, J.Mol.Model. 18 (2012) 2885–2895.
[81] D.Y. Duveau, X. Hu, M.J. Walsh, S. Shukla, A.P. Skoumbourdis, M.B. Boxer, S. V. Ambudkar, M. Shen, C.J. Thomas, Synthesis and biological evaluation of analogues of the kinase inhibitor nilotinib as abl and kit inhibitors, Bioorg.Med. Chem.Lett. 23 (2013) 682–686.
[82] L. Ding, F. Tang, W. Huang, Q. Jin, H. Shen, P. Wei, Design, synthesis, and biological evaluation of novel 3-pyrrolo [b] cyclohexylene-2-dihydroindolinone derivatives as potent receptor tyrosine kinase inhibitors, Bioorg.Med.Chem.Lett. 23 (2013) 5630–5633.
[83] H. Qi, L. Chen, B. Liu, X. Wang, L. Long, D. Liu, Synthesis and biological evaluation of novel pazopanib derivatives as antitumor agents, Bioorg.Med. Chem.Lett. 24 (2014) 1108–1110.
[84] S. Ravez, A. Barczyk, P. Six, A. Cagnon, A. Garofalo, L. Goossens, P. Depreux, Inhibition of tumor cell growth and angiogenesis by 7-aminoalkoxy-4-aryloxy-quinazoline ureas, a novel series of multi-tyrosine kinase inhibitors, Eur.J.Med. Chem. 79 (2014) 369–381.
[85] S. Ravez, S. Arsenlis, A. Barczyk, A. Dupont, R. Frédérick, S. Hesse, G. Kirsch, P. Depreux, L. Goossens, Synthesis and biological evaluation of di-aryl urea derivatives as c-kit inhibitors, Bioorg.Med.Chem. 23 (2015) 7340–7347.
[86] Y. Jin, K. Ding, D. Wang, M. Shen, J. Pan, Novel thiazole amine class tyrosine kinase inhibitors induce apoptosis in human mast cells expressing D816V KIT mutation, Cancer Lett. 353 (2014) 115–123.
[87] S. Lee, H. Lee, J. Kim, S. Lee, S.J. Kim, B.-S. Choi, S.-S. Hong, S. Hong, Development and biological evaluation of potent and selective c-KITD816V inhibitors, J.Med.Chem. 57 (2014) 6428–6443.
[88] H. Park, S. Lee, S. Lee, S. Hong, Structure-based de novo design and identification of D816V mutant-selective c-KIT inhibitors, Organ.Biomol.Chem. 12 (2014) 4644–4655.
[89] P. Chaudhari, S. Bari, In silico exploration of c-KIT inhibitors by pharmaco-informatics methodology: pharmacophore modeling, 3D QSAR, docking studies, and virtual screening, Mol.Divers. 20 (2016) 41–53.
[90] Q. Wang, F. Liu, B. Wang, F. Zou, C. Chen, X. Liu, A. Wang, S. Qi, W. Wang, Z. Qi, Discovery of N-(3-((1-Isonicotinoylpiperidin-4-yl) oxy)-4-methylphenyl)-3-(trifluoromethyl) benzamideCHMFL-KIT-110) as a selective, potent, and orally available type II c-KIT kinase inhibitor for gastrointestinal stromal tumors (GISTs), J.Med.Chem. 59 (2016) 3964–3979.
[91] Q. Wang, F. Liu, B. Wang, F. Zou, Z. Qi, C. Chen, K. Yu, C. Hu, S. Qi, W. Wang, Discovery of 4-methyl-N-(4-((4-methylpiperazin-1-yl) methyl)-3-(trifluoromethyl) phenyl)-3-((1-nicotinoylpiperidin-4-yl) oxy) benzamide (CHMFL-ABL/KIT-155) as a novelhighlypotenttype II ABL/KIT dualkinaseinhibitor with a distincthingebinding, J.Med.Chem. 60 (2017) 273–289.
[92] B. Li, A. Wang, J. Liu, Z. Qi, X. Liu, K. Yu, H. Wu, C. Chen, C. Hu, W. Wang, Discovery of N-((1-(4-(3-(3-((6, 7-Dimethoxyquinolin-3-yl) oxy) phenyl) ureido)-2-(trifluoromethyl) phenyl) piperidin-4-yl) methyl) propionamide (CHMFL-KIT-8140) as a highlypotenttype II inhibitorcapable of inhibiting the T670I "Gatekeeper" mutant of cKIT kinase, J.Med.Chem. 59 (2016) 8456–8472.
[93] H. Park, S. Lee, S. Hong, Discovery of dual inhibitors for wild type and D816V mutant of c-KIT kinase through virtual and biochemical screening of natural products, J.Nat.Prod. 79 (2016) 293–299.
[94] Z. Huang, H. Li, Q. Zhang, F. Lu, M. Hong, Z. Zhang, X. Guo, Y. Zhu, S. Li, H. Liu, Discovery of indolinone-based multikinase inhibitors as potential therapeutics for idiopathic pulmonary fibrosis, ACS Med.Chem.Lett. 8 (2017) 1142–1147.
[95] Y. Lu, F. Mao, X. Li, X. Zheng, M. Wang, Q. Xu, J. Zhu, J. Li, Discovery of potent, selectivestemcellfactor Receptor/Platelet derivedgrowthfactorreceptoralphac-KIT/PDGFRα) Dual Inhibitor for the Treatment of Imatinib-Resistant Gastrointestinal Stromal Tumors (GISTs), J.Med.Chem. 60 (2017) 5099–5119.
[96] J.G. Kettle, R. Anjum, E. Barry, D. Bhavsar, C. Brown, S. Boyd, A. Campbell, K. Goldberg, M. Grondine, S. Guichard, Discovery of N-(4-{[5-Fluoro-7-(2-methoxyethoxy) quinazolin-4-yl] amino} phenyl)-2-[4-(propan-2-yl)-1 H-1, 2, 3-triazol-1-yl] acetamide (AZD3229), a potentpan-KITmutantinhibitor for the treatment of gastrointestinalstromaltumors, J.Med.Chem. 61 (2018) 8797–8810.
[97] X. Li, Y. Huang, J. Cheng, L. Zhang, F. Mao, J. Zhu, C. Sheng, J. Li, Discovery of novel Syk/PDGFR-α/c-kit inhibitors as multi-targeting drugs to treat rheumatoid arthritis, Bioorg.Med.Chem. 26 (2018) 4375–4381.
[98] T.-S. Wu, W.-H. Lin, H.-J. Tsai, C.-C. Hsueh, T. Hsu, P.-C. Wang, H.-Y. Lin, Y.-H. Peng, C.-T. Lu, L.-C. Lee, Discovery of conformational control inhibitors switching off the activated c-KIT and targeting a broad range of clinically relevant c-KIT mutants, J.Med.Chem. 62 (2019) 3940–3957.
[99] L. Quattrini, V. Coviello, S. Sartini, T. Di Desidero, P. Orlandi, Y.-Y. Ke, K.-L. Liu, H.-P. Hsieh, G. Bocci, C. La Motta, Dual Kit/Aur inhibitors as chemosensitizing agents for the treatment of melanoma: design, synthesis, docking studies and functional investigation, Sci.Rep. 9 (2019) 1–10.
[100] X. Liu, B. Wang, C. Chen, Z. Qi, F. Zou, J. Wang, C. Hu, A. Wang, J. Ge, Q. Liu, Discovery of (E)-N 1-(3-fluorophenyl)-N 3-(3-(2-(pyridin-2-yl) vinyl)-1 H-indazol-6-yl) malonamide (CHMFL-KIT-033) as a novel c-KIT T670I mutant selective kinase inhibitor for Gastrointestinal Stromal Tumors (GISTs), J. Med. Chem. 62 (2019) 5006–5024.
[101] H. Sun, L. Zhuo, H. Dong, W. Huang, N. She, Discovery of 8-amino-substituted 2-phenyl-2, 7-naphthyridinone derivatives as new c-kit/vegfr-2 kinase inhibitors, Molecules 24 (2019) 4461.
[102] Y. Wu, B. Wang, J. Wang, S. Qi, F. Zou, Z. Qi, F. Liu, Q. Liu, C. Chen, C. Hu, Discovery of 2-(4-Chloro-3-(trifluoromethyl) phenyl)-N-(4-((6, 7-dimethoxyquinolin-4-yl) oxy) phenyl) acetamide (CHMFL-KIT-64) as a novel orally available potent inhibitor against broad-spectrum mutants of c-KIT kinase for gastrointestinal stromal tumors, J.Med.Chem. 62 (2019) 6083–6101.

[103] W.-H. Lin, S.-Y. Wu, T.-K. Yeh, C.-T. Chen, J.-S. Song, H.-Y. Shiao, C.-C. Kuo, T. Hsu, C.-T. Lu, P.-C. Wang, Identification of a multitargeted tyrosine kinase inhibitor for the treatment of gastrointestinal stromal tumors and acute myeloid leukemia, J.Med.Chem. 62 (2019) 11135–11150.

[104] A. Martorana, A. Lauria, Design of antitumor drugs targeting c-kit receptor by a new mixed ligand-structure based method, J.Mol.Graph.Model. 100 (2020), 107666.

[105] T. Roy, S.T. Boateng, S. Banang-Mbeumi, P.K. Singh, P. Basnet, R.-C. N. Chamcheu, F. Ladu, I. Chauvin, V.S. Spiegelman, R.A. Hill, Identification of new fisetin analogs as kinase inhibitors: data on synthesis and anti-skin cancer activities evaluation, Data Brief 35 (2021), 106858.

[106] T. Roy, S.T. Boateng, S. Banang-Mbeumi, P.K. Singh, P. Basnet, R.-C. N. Chamcheu, F. Ladu, I. Chauvin, V.S. Spiegelman, R.A. Hill, Synthesis, inverse docking-assisted identification and in vitro biological characterization of flavonol-based analogs of fisetin as c-kit, CDK2 and mTOR inhibitors against melanoma and non-melanoma skin cancers, Bioorg.Chem. 107 (2021), 104595.